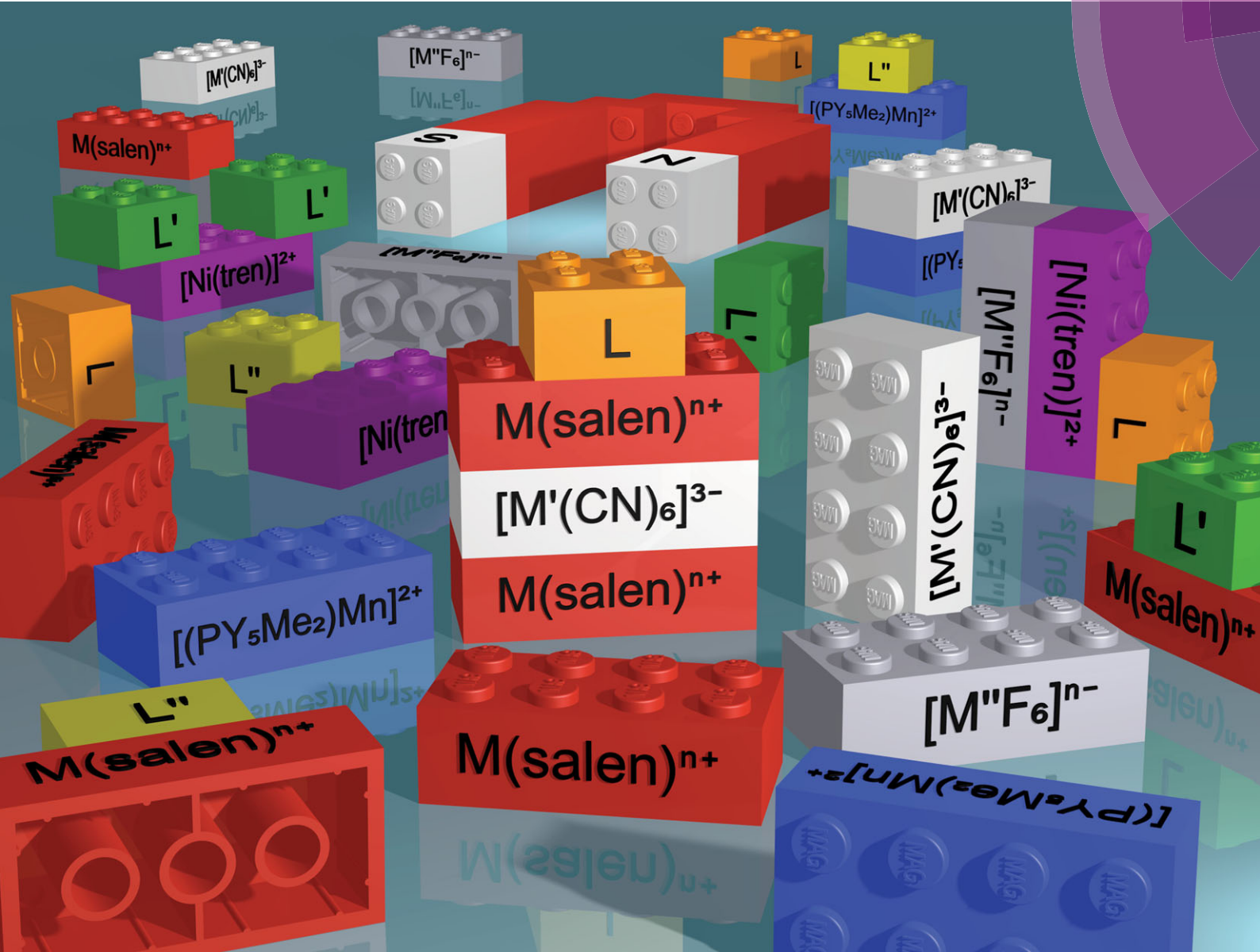


ChemComm

Chemical Communications

www.rsc.org/chemcomm



ISSN 1359-7345



FEATURE ARTICLE

Kasper S. Pedersen, Jesper Bendix and Rodolphe Clérac
Single-molecule magnet engineering: building-block approaches

Single-molecule magnet engineering: building-block approaches[†]

Kasper S. Pedersen,^{*abc} Jesper Bendix^{*c} and Rodolphe Clérac^{*ab}

Cite this: *Chem. Commun.*, 2014, 50, 4396

Received 15th January 2014,
Accepted 20th February 2014

DOI: 10.1039/c4cc00339j

www.rsc.org/chemcomm

Tailoring the specific magnetic properties of any material relies on the topological control of the constituent metal ion building blocks. Although this general approach does not seem to be easily applied to traditional inorganic bulk magnets, coordination chemistry offers a unique tool to delicately tune, for instance, the properties of molecules that behave as "magnets", the so-called single-molecule magnets (SMMs). Although many interesting SMMs have been prepared by a more or less serendipitous approach, the assembly of predesigned, isolatable molecular entities into higher nuclearity complexes constitutes an elegant and fascinating strategy. This Feature article focuses on the use of *building blocks* or *modules* (both terms being used indiscriminately) to direct the structure, and therefore also the magnetic properties, of metal ion complexes exhibiting SMM behaviour.

1. Introduction

Single-molecule magnets (SMMs), *i.e.* paramagnetic molecules exhibiting a magnet behaviour,[‡] of intrinsic molecular origin in

^a CNRS, CRPP, UPR 8641, F-33600 Pessac, France. E-mail: clerac@crpp-bordeaux.cnrs.fr;
Fax: +33 5 56 84 56 00; Tel: +33 5 56 84 56 50

^b Univ. Bordeaux, CRPP, UPR 8641, F-33600 Pessac, France

^c Department of Chemistry, University of Copenhagen, Denmark.
E-mail: ksp@kku.dk, bendix@kku.dk

[†] Dedicated to Professor Marius Andruh on the occasion of his 60th birthday.

[‡] In this report, a magnet is defined as a system exhibiting magnetic bistability, *i.e.* an M vs. H hysteresis loop.

the absence of a magnetic order, have received considerable attention in chemistry, physics and materials science since their discovery in the early 1990s.^{1–5} The main interest arose from the possible applications of SMMs in data storage, quantum computing⁶ and molecule-based spintronics devices.^{7–9} Even if SMMs have not yet been employed for practical applications, their underlying physics and chemistry have a much broader perspective. For instance, these "nanomagnets" and related molecular magnetic complexes serve as simple models for understanding more complex magnetic materials (extended 1D, 2D or 3D networks, large aggregates, . . .). Moreover, significant advancements in nanostructuring and deposition of single molecules



Kasper S. Pedersen

include synthesis and investigations of molecule-based magnetic materials based on heavier transition elements and f-elements as well as spectroscopic investigations.



Jesper Bendix

Jesper Bendix (b. in 1965, Copenhagen, Denmark) received his PhD at the University of Copenhagen under the supervision of Prof. C. E. Schäffer in 1998. Following post-doctoral stays in Mülheim, Germany with Prof. K. Wieghardt, at Caltech, USA, with Prof. H. B. Gray, at the University of Utah with Prof. J. S. Miller, and in Berne, Switzerland, with Dr P. L. W. Tregenna-Piggott (✉), he returned to Copenhagen where he is currently heading the section for inorganic chemistry. His current research focuses on synthesis as well as electronic and structural studies of molecule-based magnetic materials and on the electronic structure of high-valent metal centres.

allowed the studies on individual SMMs and to probe their intrinsic magnetic properties outside the crystal lattice.^{10,11} These detailed studies of the SMM properties include the seminal observation of slow relaxation¹² and quantum tunnelling¹³ of magnetization of magnetically isolated molecules covalently grafted to surfaces. Furthermore, studies of SMMs in solution,^{14,15} as well as nanostructured on surfaces,^{10,11,16,17} in junctions,¹⁸ films,¹⁹ porous materials²⁰ or in multi-dimensional coordination networks have been undertaken.^{21–25}

Key to the possible applications of molecular magnetic systems is a thorough understanding of the design pathways towards specific structural motifs and the understanding of the related magnetic properties of the constituent molecular entities. SMMs can be roughly divided into two classes: mononuclear and polynuclear complexes. Mononuclear SMMs have only been reported in recent years with the first example being the $[\text{Ln}(\text{pc})_2]^-$ ($\text{Ln} = \text{Dy}^{\text{III}}, \text{Tb}^{\text{III}}, \text{H}_2\text{pc} = \text{phthalocyanine}$) “double decker” complexes.²⁶ After this ground-breaking discovery, a multitude of mononuclear lanthanide,^{27–38} and more recently, several 3d metal ion complexes behaving as SMMs have been reported.^{39–45,46–48} Additionally, SMM behaviour in photo-excited spin-crossover complexes has very recently also been reported.^{49,50} Common to the majority of these systems, the slow-relaxation of magnetization arises due to a strong uniaxial magnetic anisotropy of the paramagnetic metal ion. The second class of SMMs encompasses polynuclear, exchange coupled complexes in which the constituent metal ions may be transition metal ($nd, n = 3$ to 5) ions, lanthanides/actinides ($nf, n = 4, 5$), or both. The SMM signature was reported for the first time in a dodecanuclear $\{\text{Mn}_{12}\}$ complex that is the archetypal example of an exchange-coupled polynuclear SMM.^{1,5,51,52} This family of SMMs can be further sub-divided into two classes based on the employed synthetic approach. The synthesis of the first sub-class proceeds *via* a concerted association of metal ions

through bridging ligands and with capping ligands to prevent polymerisation. The bridging ligands, most commonly oxide, hydroxide, alkoxides or phenolates obtained by deprotonation in the reaction medium, give pathways for magnetic exchange interactions between the constituent metal ions in the final polynuclear complex. The vast majority of SMMs have been obtained by this more or less serendipitous method⁵³ and pivotal studies, which have paved the way for the current understanding of SMM physics (*e.g.* quantum tunneling of magnetization, QTM,⁵⁴ and quantum coherence⁵⁵), were discovered in such systems. Alternatively, the synthetic approach towards the second sub-class of polynuclear SMMs makes use of pre-designed molecular building-blocks, which are able to associate directly in solution. In that respect, two kinds of precursors exist, namely M–L ligand donors and M' ligand acceptors, which react and form M–L–M' motifs.

The remaining and non-trivial question is now: how to define a building-block and to understand how the structure of the building-blocks influences the final polynuclear complex topology and eventually the magnetic properties? If these questions can be satisfactorily answered, SMMs can be tailored to specific applications by chemical design. In this Feature article, we review the recent efforts to design SMMs using *building-block approaches*. Instead of a comprehensive review of the vast literature, we have been selective and discuss several explanatory examples of different uses of building-blocks with various bridging ligands.

In most of the cases, the observation of an SMM behaviour is attributed to the presence of a large spin ground state (S_T) and a strong easy-axis magnetic anisotropy.⁵⁶ The large spin ground state is secured by the magnetic superexchange mechanism, which couples constituent spin centres (S_i), more or less strongly as described by the phenomenological Heisenberg–Dirac–van Vleck (HDvV) spin-Hamiltonian:

$$\hat{H} = -2 \sum_{i < j} J_{ij} \hat{\mathbf{S}}_i \cdot \hat{\mathbf{S}}_j \quad (1)$$

where J_{ij} is the interaction parameter representing ferro- or antiferro-magnetic interactions (positive and negative values, respectively) between the i th and j th spins. § In simple systems (like most of the 3d-based SMMs), the magnetic anisotropy, commonly referred to the (axial) zero-field splitting (ZFS) of the resulting ground state spin, S_T , is described by $D\hat{S}_Z^2$ where \hat{S}_Z projects S_T on the quantization (Z) axis with the eigenvalue of M_S , and D is the anisotropy parameter arising as a tensorial sum of single-ion contributions of the intrinsic local anisotropy of the metal ion units.⁵⁶ Commonly, the single ion anisotropy mainly originates from the orbital angular momentum of excited states, which is mixed into the ground state by second-order spin-orbit coupling.⁵⁶ For $D < 0$, an energy barrier (Δ) of DS_T^2 (for integer S_T) or $\Delta = D(S_T^2 - 1/4)$ (for half-integer S_T) separates

§ Alternative Hamiltonian conventions (as a matter of personal taste) such as $-\sum_{i < j} J_{ij} \hat{\mathbf{S}}_i \cdot \hat{\mathbf{S}}_j$ or $\sum_{i < j} J_{ij} \hat{\mathbf{S}}_i \cdot \hat{\mathbf{S}}_j$ are often found in the literature and a special attention to the employed definition should be given when comparing parameter values. Throughout this Feature article, we will consistently adopt the definition given in eqn (1).



Rodolphe Clérac

Texas, USA) where he collaborated with Prof. F. A. Cotton. In 2000, he established his research group (Molecular Materials & Magnetism) at the Centre de Recherche Paul Pascal (CNRS) interested in the synthesis and physical properties of molecular materials.



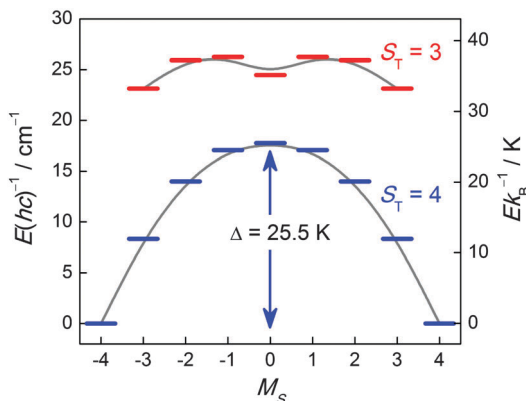


Fig. 1 Energy level diagram of the two lowest spin-multiplets of an $S_T = 4$ SMM ($[\text{Mn}^{\text{III}}_2(\text{saltmen})_2(\text{ReO}_4)_2]$) from ref. 61 (saltmen = N,N' -1,1,2,2-tetramethylethylenebis(salicylideneiminate)). The energy level diagram was calculated with $J_{\text{Mn}-\text{Mn}}/k_{\text{B}} = +2.7$ K and $D/k_{\text{B}} = -4.0$ K. Only the two energetically lowest spin manifolds are shown and solid lines are a guide for the eye.

the $M_S = \pm S_T$ ground states. Recently, a few examples of mononuclear systems exhibiting $D > 0$ were reported to exhibit SMM properties; however, the underlying physics is still in debate.^{57–60} An energy diagram of an SMM with an easy-axis anisotropy ($D < 0$) is schematized in Fig. 1.⁶¹ The energy span of the $S_T = 4$ manifold resulting from ferromagnetic coupling of two $S = 2$ Mn^{III} centres has an energy barrier from $M_S = \pm 4$ to $M_S = 0$ of $\Delta/k_{\text{B}} = 25.5$ K.⁶¹ By application of a magnetic field, one of the two “wells” can be stabilized and thereby selectively populated due to the Zeeman energy $\mu_{\text{B}}g_ZH_ZM_S$ (with the field applied along the quantization, Z , axis). When the polarizing field is removed, the system is magnetized and out of equilibrium. In a thermally activated regime where the relaxation is due to spin–phonon interaction, the magnetization of the system follows an exponential decay: $M(t) = M(t = 0) \times \exp(-t/\tau)$. This expression also defines the relaxation time, τ , that obeys a thermally activated behaviour, *i.e.* the Arrhenius law: $\tau(T) = \tau_0 \exp[\Delta/(k_{\text{B}}T)]$.² The magnitude of the energy barrier, Δ , and the pre-exponential factor, τ_0 , which is related to, for instance, the nature of the spin–phonon interaction,[¶] are the characteristic parameters commonly reported for an SMM. Most of

¶ It is worth noting that in most of the cases, τ_0 is not easy to estimate accurately for a few reasons: (i) it is not always experimentally possible to obtain a clear (*i.e.* linear) thermally activated behavior of the relaxation time over many decades of time (that requires different experimental setups); there is often some kind of curvature in $\ln(\tau)$ vs. T^{-1} (likely originating from additional relaxation mechanisms) if the measurements cannot reach sufficiently high temperatures; (ii) τ_0 is also strongly influenced by the “bath”, *i.e.* the environment, in which the magnetization of the SMMs slowly relaxes. For example, weak magnetic coupling between SMMs influence τ_0 as illustrated in chains of SMMs or SCM systems in which τ_0 is also thermally activated and function of the intra-chain interactions; (iii) in some systems, which display a very broad spectrum of energy, multiple relaxation processes can be explored increasing the temperature and thus τ_0 might change depending of the relaxation process explored. Quite generally, τ_0 should be of the order of 10^{-10} to 10^{-12} s to be compatible with typical vibrations of the network that govern the reversal of magnetization. In many SMM examples, τ_0 is reported to be larger and sometimes much larger than 10^{-10} s, suggesting that additional effects are indeed hidden in this parameter.

the time, an experimental “effective” barrier (Δ_{eff}) smaller than the expected one (Δ , on the basis of S_T and D) is obtained due to quantum tunnelling of magnetization (QTM) through the potential barrier *via* excited M_S states.² Indeed this is the case of the above example (Fig. 1) for which the observed energy barrier (Δ_{eff}) extracted from ac susceptibility measurements is only 16 K, which is much lower than the calculated value (25.5 K). However, application of a small dc field (800 Oe) puts the $\pm M_S$ levels out of resonance and thereby increases Δ_{eff} to 23 K. The QTM is governed by non-diagonal terms entering into the Hamiltonian, giving rise to a mixing of M_S states. In the vast majority of the characterized SMMs, the symmetry is lower than axial and the anisotropy part of the spin Hamiltonian to second order reads $\hat{H} = D(\hat{S}_Z^2 - \frac{1}{3}S_T(S_T + 1)) + E(\hat{S}_X^2 - \hat{S}_Y^2)$ where $|E| \leq \frac{1}{3}|D|$. The E term has the effect of mixing the M_S states differing by $\Delta M_S = \pm 2$. In some cases, this anisotropy description might not be sufficient to explain the relaxation and thus higher order terms, despite their small parameter values, have to be taken into account.²

For the reasons stated above, the maximization of both D and S_T seems crucial for the successful preparation of SMMs. Synthetically, it has been proven very difficult to obtain a large S_T ground state by ferromagnetic interactions whilst simultaneously perfectly aligning anisotropy axes of each magnetic site. The largest SMM reported to date is an aesthetic $\{\text{Mn}^{\text{III}}_{84}\}$ nanoscopic wheel which, despite its high nuclearity, exhibits only a relatively small spin ground state of ~ 6 and a modest energy barrier of 18 K.⁶³ The largest S_T is found in a ferromagnetically coupled mixed-valence $\{\text{Mn}^{\text{II}}_7\text{Mn}^{\text{III}}_{12}\}$ complex exhibiting a record $S_T = 83/2$ ground state but no SMM properties are observed due to an almost perfect compensation of the Mn^{III} local anisotropy tensors.^{64,65} One of the successes in the realm of polynuclear SMMs has been a family of $\{\text{Mn}_6\}$ complexes, some of which exhibit an energy barrier higher ($\Delta_{\text{eff}}/k_{\text{B}} = 86.4$ K for $[\text{Mn}^{\text{III}}_6\text{O}_2(\text{Et-sao})_6(\text{O}_2\text{CPh}(\text{Me}))_2(\text{EtOH})_6]$, Et-saoH₂ = 2-hydroxyphenylpropanone oxime) than the celebrated $\{\text{Mn}_{12}\}$ SMM ($\Delta_{\text{eff}}/k_{\text{B}} = 61$ K).^{1,66,67} Indeed targeting very large spin ground states in pursuit of effective SMMs is not necessarily the most fruitful approach since the overall anisotropy decreases as S_T^{-2} , leading to a SMM energy barrier almost independent of S_T for sufficiently large S_T values.^{68–70} Recently, M vs. H hysteresis loops at unprecedented temperatures (up to 14 K, 0.9 mT s⁻¹) have been reported for dinuclear lanthanide complexes bridged by the exotic paramagnetic N_2^{3-} radical,^{71,72} and a record anisotropy barrier for polynuclear SMMs of more than 600 K was observed for a $\{\text{Dy}_4\text{K}_2\}$ hexanuclear complex.^{||}⁷³ Particularly in the latter case, these promising results rely rather on the strong single-ion magnetic anisotropy of the lanthanide ions than on the spin ground state of the molecule. However, the use of spin architectures employing multiple spin centres remains a viable route to prepare individual molecules with interesting

|| In this context, the experimental estimation of Δ_{eff} by assuming a pure thermally activated process at the highest available temperatures may be inappropriate in some cases as recently demonstrated independently by Sorace, Dreiser and co-workers.^{37,38}

magnetic properties, while simultaneously exploiting and optimizing the existing knowledge of preparative coordination chemistry. Importantly, this also constitutes the most realistic approach towards a good understanding of the interaction of magnetic molecules (irrespective of their nuclearity) with extended structures, *e.g.* surfaces.

2. Topological control

The rational synthesis of polynuclear metal complexes using a bottom-up approach based on *building blocks* or *modules* is by no means a new idea nor restricted to magnetic systems.⁷⁴ However, due to the intimate relationship between structure and magnetic properties, this approach is particularly relevant for polynuclear magnetic systems. In order for the building blocks to be able to direct or template the desired structure of a polynuclear system some prerequisites need to be fulfilled to avoid the synthesis of non-expected products that might be thermodynamically favored. One of the most important aspects is to consider modules with a sufficient degree of robustness to maintain their structure-directing abilities under the assembly conditions. This somewhat vague property reflects the relative nature of the robustness concept in connection with synthesis, balancing ligand exchange kinetics between the different precursors and with the harshness of the conditions required for the assembly of the targeted polynuclear system.

A second prerequisite for the building blocks to function as structure directing entities is a built-in preference for a specific coordination geometry at metal centers as well as at the bridging ligands. Octahedral coordination is predominant for the transition metal ions, and this is especially true for the kinetically robust systems. For a bridging ligand, the simplest conceivable geometry is to linearly connect two metal ions. This is true for the ubiquitous cyanide bridges, but also to quite some extent for fluoride, but not for oxide, when acting as bridging ligands. This tendency is supported by the histograms of Fig. 2 showing the crystallographically determined $M-N\equiv C$ angle

(where M is a transition metal ion) and, for comparison, the $M-F/O-M'$ angles in unsupported fluoride/oxide-bridged molecules and networks. The relative numbers are striking and reflect the extensive scientific work in cyanide chemistry. Consequently, $M-N\equiv C-M'$ motifs with robust octahedral metal ions, which are reminiscent of the Prussian blue compounds,⁷⁶ are frequently used to design polynuclear complexes. Many molecular species obtained from building blocks of different denticities can be conceptually considered as fragments of a three-dimensional Prussian blue structure.⁷⁷

The robustness of a given building block can derive from either the metal center (*e.g.* the most robust ones being d^3 and diamagnetic low-spin d^6 metal ions) or from the use of polydentate, and possibly, rigid ligands. Due to the limited choice of d^3 or d^6 systems, the use of polydentate ligands is the most efficient approach to enforce robustness and additionally to allow further geometrical preferences based on ligand design.

It should be mentioned that in this Feature article, the definition of the building blocks will be restricted to a molecular entity encompassing at least one metal ion. However, in a broader perspective, it is also useful to note that a less intuitive definition of the building block concept considers a metal-free bridging ligand as a building block directing the geometry of the whole system by its robust structure. This definition significantly widens the modular description but allows for a unified view encompassing common polynuclear topologies directed by the ligand structure. This last aspect is well illustrated by the large number of ring structures obtained using bridging carboxylate ligands.⁷⁸ Indeed, the vast majority of the reported SMMs also falls in this extended definition and will not be included in this article; instead the reader is directed to excellent reviews by Aromi,³ Winpenny,⁷⁹ Christou,⁸⁰ Tang,⁸¹ and Powell⁸² for a detailed discussion of SMM topologies and their molecular control by ligand design.

In the context of molecule-based magnetism, the bridging ligand, in addition to guiding the structure, also needs to be compact enough to mediate efficient magnetic interactions. From the synthetic point of view, it is also preferable to choose bridging ligands with moderate basicity. Bridging ligands that are too reactive would limit the range of possible partners and conditions (*e.g.* solvents) since their structural integrity may be compromised, emphasizing further the relative nature of the robustness concept.

An essential aspect in engineering building blocks is to provide intrinsic magnetic characteristics essential to contribute to the final magnetic properties. To obtain SMMs, the building blocks usually contribute with Ising-like magnetic anisotropy or a large spin but other interesting additional properties like photomagnetism or luminescence can also be implemented. Building blocks may come as either homoleptic complexes, for which the cyanide (see Section 3) and oxalate (see Section 4) complexes are the most common, or as heteroleptic systems for which a large variety of ligand combination have been employed with a strong predominance of cyanide-based complexes. For the heteroleptic systems, the coordination sphere of the octahedral complexes, which can be *cis*-*trans*- or *fac*-*mer*-stereoisomers, directs towards different polynuclear structures.

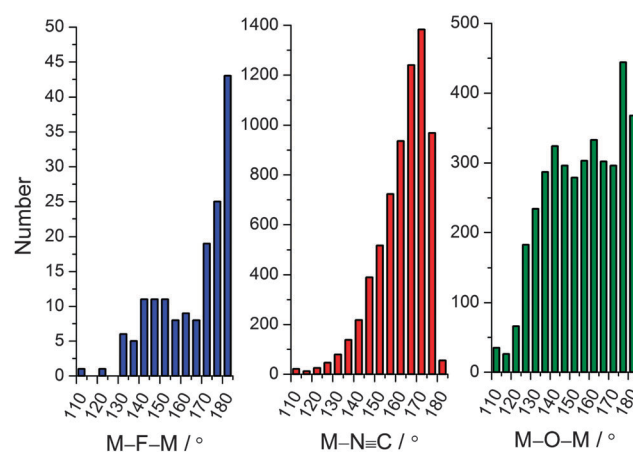


Fig. 2 Histograms showing the numbers of the structurally characterized (Cambridge Structural Database)⁷⁵ unsupported $M-F-M'$ (left), $M-N\equiv C$ (middle) and unsupported $M-O-M'$ (right) bridging angles.



The polymerization of building block units into multi-dimensional structures is a common synthetic problem for chemists who want to engineer molecular objects. In most of the cases, the successful synthesis of polynuclear complexes involves precursor units with strongly directional coordination abilities, which must be assisted by an appropriate choice of capping ligands. This choice is by no means trivial. First, the capping ligands often provide the solubility requirements for the subsequent assembly. Furthermore, the nature of the capping ligand may have dramatic structure-directing properties imposed by second coordination sphere interactions and packing effects. On the other hand, coordination polymers of SMMs are certainly another interesting research area that has led to magnetically interesting systems such as single-chain magnets (SCMs).^{21,83–86} Indeed, some SCM systems can be considered as one-dimensional polymers of SMM repeating units, allowing the modelling of the complex dynamics of Ising-type SCMs,^{22,84,87–89} on the basis of the known properties of the isolated SMMs.

3. Cyanide-based precursors

By far, the cyanide-based homo- or heteroleptic precursors are the most ubiquitous building blocks that have been used to design SMMs, high-spin or simple magnetic molecules (“0D”), extended magnetic networks such as chains (1D), sheets (2D) and three-dimensional (3D) lattices. Shatruk, Avendano and Dunbar reviewed comprehensively the chemistry of polynuclear cyanidometallates in 2009 and herein we will focus mainly on results obtained since.⁷⁶ To quote these authors: “*The shape adopted by the cyanide-bridged core in these clusters is dictated by the topology of the available coordination sites*”. This sentence describes precisely what will be the theme of the following paragraphs.⁷⁶

The interest in cyanide-based SMMs is in direct line with the famous Prussian blue and its analogues, which have been intensively studied, in particular by the groups of Girolami,⁹⁰ Verdaguer,⁹¹ and Miller.⁹² In these systems, an experimental and detailed theoretical understanding^{91,93} of the magnetic interaction through bridging cyanide ligands has been achieved in relation to the involved metal ions and structural/geometrical parameters. This knowledge of the exchange mechanisms was fundamental in order to engineer cyanide-encompassing molecular analogues with tailor-made magnetic properties. The popularity of the cyanide ion was also boosted by the availability and robustness of many cyanide complexes and the strong tendency of cyanide to bridge between transition metal centres. As discussed in the previous paragraph, cyanide often imposes an almost linear bridging mode that facilitates the design and prediction of specific topologies of the resulting polynuclear complexes. Moreover, the use of cyanide makes the heavier transition metals (4d, 5d) accessible to SMM materials. These elements exhibit some advantages over 3d metal ions as the presence of more diffused 4d/5d orbitals may give rise to stronger exchange interactions and significant magnetic anisotropy due to the strong spin-orbit coupling, as will be discussed

in the next paragraphs.^{94–96} Remarkably, some of the Prussian blue analogues have shown interesting properties such as pronounced magnetic interactions leading to high ordering temperatures,⁹⁰ charge-transfer and photomagnetic effects,⁹⁷ all of which could possibly be, or have been, realized in molecule-based systems.

Homoleptic cyanidometallates

Homoleptic cyanide-complexes are known to possess coordination numbers ranging from 2 to 8, which allow them to bridge several metal ions.^{76,98,99} In SMM syntheses, only those having 6, 7 or 8 cyanide ligands have been employed with a majority of systems based on hexacyanide complexes.^{74,100} Paramagnetic hexacyanidometallates(m), $[\text{M}(\text{CN})_6]^{3-}$ are well-known for Ti to Fe,^{101–103} Mo,¹⁰⁴ Ru,¹⁰⁵ Os,¹⁰⁶ and Ni (in solution).¹⁰⁷ This series represents a unique opportunity to systematically investigate homologous SMMs incorporating transition metal ions with different d-orbital occupations; ideally with predictable structures, magnetic anisotropies and nature of the magnetic interaction.^{93,100,108} For example, if $[\text{Cr}(\text{CN})_6]^{3-}$ is coordinated to a Ni^{II} ion through a strictly linear cyanide bridge, the magnetic interaction is of ferromagnetic nature due to the orthogonality of the spin-bearing orbitals of Cr^{III} [$t_{2g}^3(O_h)$] and those of Ni^{II} [$t_{2g}^6e_g^2(O_h)$]. However, such predictions do not necessarily guarantee the successful synthesis of ferromagnetically coupled $\text{Cr}^{\text{III}}\text{-CN-Ni}^{\text{II}}$ complexes as small deviations from idealized geometries may give rise to, at first sight, counterintuitive results.

One of the first examples of an SMM incorporating a homoleptic cyanidometallate was indeed a $\{\text{Cr}^{\text{III}}\text{Ni}^{\text{II}}_6\}$ complex: $[\text{Cr}^{\text{III}}(\text{CN})_6\{\text{Ni}^{\text{II}}(\text{tetren})\}_6(\text{ClO}_4)_9$ (**1**)¹⁰⁹ (tetren = tetraethylenepent-tetraethylenepentamine) having a *close-to-octahedral* $\{\text{Cr}^{\text{III}}(\mu\text{-CN})_6\text{Ni}^{\text{II}}_6\}$ central core. Ferromagnetic $\text{Ni}^{\text{II}}\text{-Cr}^{\text{III}}$ coupling interactions ($J_{\text{Ni-Cr}}/k_{\text{B}} = +12.1$ K) give rise to an $S_{\text{T}} = 15/2$ ground state. Even though Ni^{II} often possesses strong magnetic anisotropy, the proximity of the complex to octahedral symmetry is expected to significantly decrease the overall magnetic anisotropy and hence only a very small anisotropy barrier was found ($\Delta_{\text{eff}}/k_{\text{B}} \approx 6$ K, $\tau_0 = 1.1 \times 10^{-11}$ s).¹⁰⁰ The first established SMM incorporating a homoleptic cyanidometallate building block was a trigonal bipyramidal (TBP) complex, $\{[\text{Mn}^{\text{II}}(\text{tmpphen})_2]_3[\text{Mn}^{\text{III}}(\text{CN})_6]_2\}$ (**2**, tmpphen = 3,4,7,8-tetramethyl-1,10-phenanthroline) reported by Dunbar and co-workers.^{110,111} Herein, each of three facially-oriented cyanide ligands of the $[\text{Mn}(\text{CN})_6]^{3-}$ moiety links to a $\{\text{Mn}(\text{tmpphen})_2\}^{2+}$ unit as depicted in Fig. 3. Since the Mn^{II} magnetic anisotropy is negligibly small, the presence of a spin-relaxation barrier arises due to anisotropic $\text{Mn}^{\text{III}}\text{-Mn}^{\text{II}}$ exchange interactions through the bridging cyanides induced by the unquenched orbital angular momentum of the low-spin Mn^{III} (t_{2g}^4) in octahedral symmetry (*vide infra*).^{112,113} In 3d metal ions, the orbital angular momentum is generally quenched by the presence of a low-symmetry ligand field. However, in systems incorporating hexacyanidometallates the main perturbation of the d-orbitals arises from the strong octahedral ligand field and thereby leaves the orbital angular momentum unquenched to a large extent even in polynuclear complexes with a low overall symmetry.¹¹⁴ Dunbar and co-workers reported several other TBP



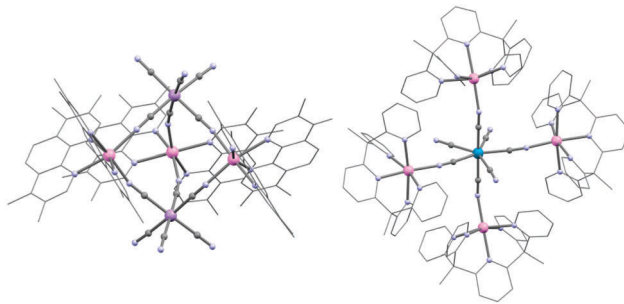


Fig. 3 Molecular structures of **2** (left) and **14** (right). Colour code: Re, maroon; Mn^{III}, purple; Mn^{II}, pink; N, blue; C, grey. The C skeleton is shown as wireframe. Hydrogens, counterions and co-crystallized solvent molecules have been omitted for clarity. The latter two sentences apply to all the figures of this Feature article.

complexes but none showing SMM properties, while on the other hand, some of them showed remarkable spin-crossover and photomagnetic behaviour.^{111,115}

The groups of Long, Miyasaka and Clérac reported similar trinuclear {Mn^{III}Fe^{III}Mn^{III}} SMMs in which two Mn^{III} Schiff-base (SB) complexes “sandwich” a *trans*-bridging [Fe(CN)₆]³⁻ moiety.^{87,116,117} In these compounds, the co-axial orientation of the Mn^{III} ZFS tensors and the ferromagnetic Mn-Fe interaction ($J_{\text{Mn-Fe}}/k_{\text{B}} = +6.5$ K) both contribute to the SMM behaviour.¹¹⁶ (NEt₄)₂[Mn₂(rac-salmen)₂-(MeOH)₂Fe^{III}(CN)₆] (**3**) (rac-salmen²⁻ = rac-(methylethylene)bis-salicylideneiminate, Fig. 4) has the higher spin-relaxation barrier ($\Delta_{\text{eff}}/k_{\text{B}}$) of 14 K ($\tau_0 = 2.5 \times 10^{-7}$ s).^{88,117,118}

The {Mn(SB)}⁺ complexes are widely used modules to design SMMs due to the relatively strong magnetic anisotropy originating

from the ZFS of the Mn^{III} (d⁴) metal ion in tetragonal ligand fields imposed by the Jahn-Teller (JT) elongation.¹¹⁹ A comprehensive discussion of the {Mn(SB)}⁺ chemistry can be found in ref. 120 and some SMM highlights are presented in the next sections. Using the synthetic approach developed for **3** with different central hexacyanidometallate moieties, an isostructural series of SMMs has been described based on [Cr(CN)₆]³⁻ (**4**),¹²¹ [Fe(CN)₆]³⁻ (**5**),¹²² [Ru(CN)₆]³⁻ (**6**),¹²³ and [Os(CN)₆]³⁻ (**7**)¹²² building blocks, “sandwiched” between two [Mn^{III}(5-Brsalen)-(MeOH)]⁺ (5-Brsalen²⁻ = ethylene-bis(5-bromosalicylidene)iminate) units. The molecular structure of the [Mn₂(5-Brsalen)₂(MeOH)₂-M(CN)₆]⁻ unit is very close to that found in K[Mn₂(5-Brsalen)₂-(H₂O)₂M(CN)₆]⁻·2H₂O^{116,118} but the presence of NEt₄⁺ counterions and methanol capping ligands on Mn^{III} ligands leads to more magnetically isolated complexes and unquestionable SMM properties. From the viewpoint of the detailed understanding of the magnetic properties, **4** is the simplest system to analyse due to the orbitally non-degenerate ground state of the [Cr(CN)₆]³⁻ building block. The Mn^{III}-Cr^{III} interaction is anti-ferromagnetic, thereby giving rise to an $S_{\text{T}} = 5/2$ ground state with a spin-relaxation barrier due to the intrinsic magnetic anisotropy provided by the Mn^{III} sites. A detailed study of this SMM combining magnetic measurements, frequency-domain Fourier-transform THz-EPR spectroscopy and inelastic neutron scattering (INS) was reported to gain insight into the low-lying energy states of **4**.¹²¹ Specifically, the analysis of both spectroscopic and magnetic data led to the following set of parameters: $J_{\text{Mn-Cr}}/k_{\text{B}} = +6.90$ K and $D/k_{\text{B}} = -5.25$ K. A similar analysis of the isostructural complex **8**, incorporating diamagnetic [Ir(CN)₆]³⁻, yielded $D_{\text{Mn}}/k_{\text{B}} = -5.35$ K and $E_{\text{Mn}}/k_{\text{B}} = +0.30$ K demonstrating that the intrinsic properties of the {Mn(SB)}⁺ unit are unaltered.¹²⁴ Complex **4** displays clear frequency-dependent maxima in the out-of-phase component of the dynamic (ac) susceptibility with an SMM energy barrier of 18 K ($\tau_0 = 2 \times 10^{-8}$ s), which is slightly lower than the spectroscopically determined value of 26 K. This observation might be the result of QTM *via* the first excited state located at 18 K ($M_S = \pm 3/2$, $S_{\text{T}} = 5/2$). In **5**–**7**, the theoretical treatment is more complicated as the exchange interactions become largely anisotropic as a result of the first-order orbital angular momentum present within the ground $^2\text{T}_{2g}(nd^5)$ term (O_{h}).^{114,125–127} The transformation properties of the orbital angular momentum operator, \hat{L} , leads to non-zero matrix elements, $\langle \Gamma | \hat{L} | \Gamma \rangle$, only for $\Gamma = ^{2S+1}\text{T}_{1g}$ or $^{2S+1}\text{T}_{2g}$.¹²⁸ Importantly, the orbital contributions to the superexchange mechanism render the HDvV Hamiltonian inapplicable.^{114,125} For $^2\text{T}_{2g}(nd^5)$, the strong coupling of the fictitious $l = 1$ orbital momentum associated with a T term and the $S = 1/2$ spin momentum, lifts the 6-fold degeneracy giving a lower-lying $E'_{1g(1/2)}$ Kramers doublet ($j = 1/2$) of the octahedral double group (O_{h}^*).¹²⁸ Taking **7** as an example, the simultaneous modelling of the dc susceptibility, magnetization, INS and frequency-domain Fourier-transform EPR spectra by means of a nearest neighbour spin-Hamiltonian yielded the following principal component parameters $J_{xx}/k_{\text{B}} = 13(1)$ K, $J_{yy}/k_{\text{B}} = -25(1)$ K and $J_{zz}/k_{\text{B}} = 24(1)$ K.¹²⁹ The averaged parameters show an increase in the values extracted for the isostructural complex **6**,

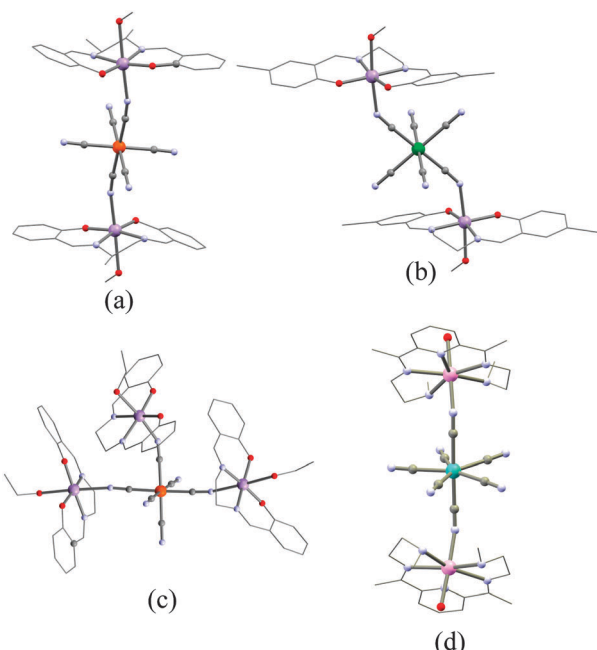


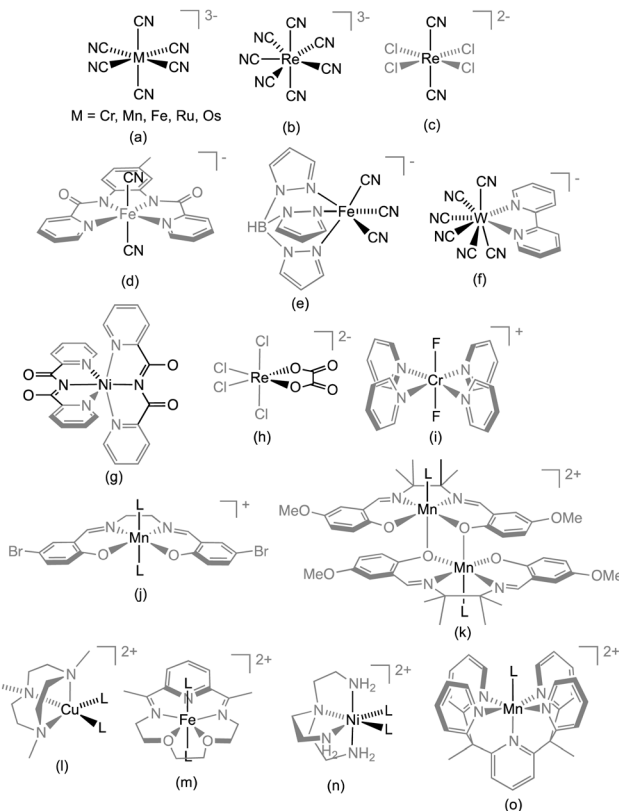
Fig. 4 Molecular structures of **3** (a), **7** (b), **9** (c) and **19** (d). The main structural difference between **3** and **7** lies in the Mn–N–C angle being 165° and 145° degrees, respectively. Colour code: Os, green; Mo, turquoise; Mn^{III}, purple; Mn^{II}, pink; Fe, orange; O, red; N, blue; C, grey.



incorporating $[\text{Ru}(\text{CN})_6]^{3-}$, corroborating the common theorem that descending in a transition metal group gives rise to an increase in the magnetic interaction due to increasingly diffuse magnetic orbitals.^{94,95,130} The energy separation between the ground $j = 1/2$ doublet and $j = 3/2$ state is given by $\frac{3}{2}\zeta_{nl}$, where ζ_{nl} is the one-electron spin-orbit coupling parameter. ζ_{nl} scales dramatically with the atomic number and is approximately 700 and 4000 K for Fe and Os, respectively.¹³¹ When $[\text{M}(\text{CN})_6]^{3-}$ building blocks are parts of a polynuclear complex, the symmetry is no longer octahedral and low-symmetry ligand field effects become often of importance. For the $[\text{Os}(\text{CN})_6]^{3-}$ unit that exhibits a strong ligand field of $\Delta_O/k_B \approx 56\,000$ K ($\sim 39\,000\text{ cm}^{-1}$),¹⁰⁶ small ligand field effects are unlikely to alter the $j = 1/2$ ground state or induce significant quantum mixing as the separation from the $j = 3/2$ state is quite large: $\frac{3}{2}\zeta_{\text{Os}^{(\text{III})}} \approx 6000$ K. For lighter atoms such as Fe^{II} in a $[\text{Fe}(\text{CN})_6]^{3-}$ environment, small ligand field effects are able to mix $j = 3/2$ into the ground state. Using the angular overlap model, Tregenna-Piggott *et al.* estimated the $^2\text{T}_{2g}$ energy splitting of a $\{\text{Fe}(\text{CN})_6\}^{3-}$ *trans*-bridging unit to yield three Kramers doublets at 0, 850 and 1450 K.¹¹⁶ The intrinsic complicated magnetic properties of the $[\text{Fe}(\text{CN})_6]^{3-}$ and $[\text{Mn}(\text{CN})_6]^{3-}$ building blocks and their unexplored $[\text{V}(\text{CN})_6]^{3-}$ and $[\text{Ti}(\text{CN})_6]^{3-}$ analogues, make them less predictable – but fascinating – magnetic modules to design SMMs.¹³² Interestingly, Δ_{eff} for complexes 5 to 7 was found to increase upon descending in the group 8 of the periodic table, emphasizing the promising and largely unexplored properties of 4d and 5d metals in the quest for new SMMs.¹³³

Related to the above systems based on $\{\text{Mn}(\text{SB})\}^+$ units, a “T-shaped” SMM, $[\text{Mn}^{\text{III}}(\text{salen})(\text{EtOH})_3][\text{Fe}^{\text{III}}(\text{CN})_6]$ (9, Fig. 4c) was also reported (salen²⁻ = *N,N'*-ethylene-bis(salicylidene-iminate)).¹³⁴ The nearly perpendicular orientation of the Mn^{III} JT axes reduces the overall magnetic anisotropy and the complex has a smaller energy barrier than the related system 3. When the assembly of $\{\text{Mn}(\text{SB})\}^+$ and $[\text{Cr}(\text{CN})_6]^{3-}$ is pursued to its logical end, a heptanuclear complex is formed, $[\text{Cr}(\mu\text{-CN})_6\text{Mn}^{\text{III}}_6(\text{salen})_6(\text{EtOH})_6]$ (10).¹¹⁹ For this complex, the nearly complete cancellation of D by the almost perpendicular JT axes results in the absence of SMM behaviour. The $[\text{Cr}(\text{CN})_6]^{3-}$ module was also combined with an $S = 2$ Fe^{II} ion placed in a macrocyclic pentadentate ligand yielding a linear ferromagnetically ($J_{\text{Fe-Cr}}/k_B = 5.41$ K) coupled $\{\text{Fe}^{\text{II}}_2\text{Cr}^{\text{III}}\}$ complex (11, $\{\{\text{Fe}(\text{LN}_3\text{O}_2)(\text{H}_2\text{O})_2\}_2\text{Cr}(\text{CN})_6\}[\text{ClO}_4] \cdot 3\text{H}_2\text{O}$; $\text{LN}_3\text{O}_2 = 3,12,18\text{-triaza-6,9-dioxabicyclo[12.3.1]octadeca-1(18),14,16-triene}$) with a large $\Delta_{\text{eff}}/k_B = 44.3$ K ($\tau_0 = 1.4 \times 10^{-9}$ s).¹³⁵ The magnetic anisotropy in this SMM originates from the hepta-coordinated Fe^{II} ($S = 2$) unit (see Scheme 1m) for which D_{Fe}/k_B amounts to -6.7 K.

Glaser *et al.* extended the hexacyanidometallate approach by exploiting phloroglucinol-derived (= 1,3,5-trihydroxybenzene) salen ligands to synthesize a heptanuclear $\{\text{Mn}^{\text{III}}_6\text{Cr}^{\text{III}}\}$ SMM (12, Fig. 5, $[(\text{talen}^{\text{Bu}_2})\text{Mn}_3]_2[\text{Cr}(\text{CN})_6](\text{MeOH})_3(\text{CH}_3\text{CN})_2](\text{BPh}_4)_3 \cdot 4\text{CH}_3\text{CN} \cdot 2\text{Et}_2\text{O}$; $\text{H}_6\text{talen}^{\text{Bu}_2} = 2,4,6\text{-tris}\{1\text{-[2-(3,5-di-}tert\text{-butylsalicylaldimino)-2-methylpropylimino]-ethyl}\}\text{-1,3,5-trihydroxybenzene}$) exhibiting an effective barrier of 25.4 K.^{136,137} The main difference of this system from 10 lies in a trigonal distortion of the octahedral geometry resulting in a non-cancellation of the magnetic



Scheme 1 Representative examples of donor-type (a–i) and acceptor-type modules (j–o), which have all been employed to design SMMs. For the latter type, “L” designates the accessible coordination site(s).

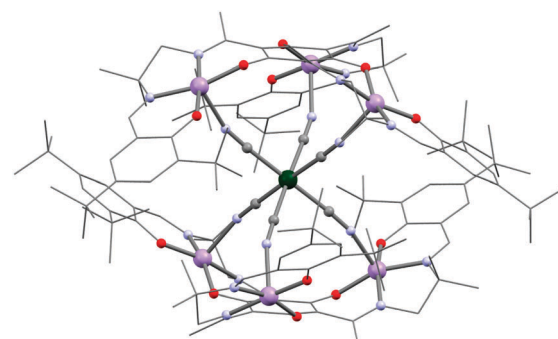


Fig. 5 Molecular structure of 12. Solvent molecules located on axial 6th position of the Mn^{III} sites and counterions have been omitted for clarity. Colour code: Mn, purple; Cr, dark green; O, red; N, pale blue; C, grey.

anisotropy and thereby in the observation of the SMM behaviour.¹³⁷ Fitting of the χT vs. T data at high temperatures allowed an estimation of $J_{\text{Mn-Cr}}$ at about -7.2 K (with $S_{\text{T}} = 21/2$). This value is close to the one found for 4 despite the more linear Mn–N–C angle of $160\text{--}162^\circ$ in 12. The synthesis of C_3 symmetrical SMMs is particularly appealing as the QTM is commonly governed by the rhombic E term that vanishes in the trigonal symmetry. Nevertheless, higher order terms of the anisotropy allowed in the C_3 symmetry might still govern the QTM despite their small values. Exchanging $[\text{Cr}(\text{CN})_6]^{3-}$ by



$[\text{Fe}(\text{CN})_6]^{3-}$ affords the analogous $\{\text{Mn}^{\text{III}}_6\text{Fe}^{\text{III}}\}$ complex showing weak characteristics of SMM behaviour.¹³⁸ However, substituting for $[\text{Os}(\text{CN})_6]^{3-}$ yields $\{\text{Mn}^{\text{III}}_6\text{Os}^{\text{III}}\}$ with stronger anisotropy and slower relaxation of the magnetization due to anisotropic $\text{Mn}^{\text{III}}\text{-Os}^{\text{III}}$ exchange interactions.¹³⁹

Recently, the same group reported an analogous $\{\text{Mn}^{\text{III}}_6\text{Mn}^{\text{III}}\}$ complex encompassing a central low-spin $[\text{Mn}(\text{CN})_6]^{3-}$ module ($\{[(\text{talen}^{\text{Bu}2})(\text{Mn}^{\text{III}}(\text{MeOH}))_3]_2\{\text{Mn}^{\text{III}}(\text{CN})_6\}\}(\text{lac})_3\cdot 10.5\text{MeOH}$, **13**, lac⁻ = lactate).¹⁴⁰ Thanks to the lactate counterions that favour the occurrence of hexagonal and cubic packings, the $\{\text{Mn}^{\text{III}}_6\text{Mn}^{\text{III}}\}$ complex adopts an *S*₆ crystallographic symmetry. Notably, a trigonal distortion of $[\text{Mn}(\text{CN})_6]^{3-}$ does not quench the effective *l* = 1 orbital angular momentum but the spin-orbit coupling leads to a nonmagnetic ground state for the *j* = 0 $[\text{Mn}(\text{CN})_6]^{3-}$ central unit.^{140,141} Despite the “blocked” exchange pathway through the essentially diamagnetic $[\text{Mn}(\text{CN})_6]^{3-}$ unit (at low temperature), the $\{\text{Mn}^{\text{III}}_6\text{Mn}^{\text{III}}\}$ complex exhibits an unusual double *M* vs. *H* hysteretic behaviour. The weak intra- $\{\text{talen}^{\text{Bu}2}\text{Mn}^{\text{III}}_3\}$ $\text{Mn}^{\text{III}}\text{-Mn}^{\text{III}}$ antiferromagnetic interactions stabilize an *S* = 2 intermediate spin state for both $\{\text{talen}^{\text{Bu}2}\text{Mn}^{\text{III}}_3\}$ units, which interact weakly ferromagnetically leading to an *S_T* = 4 ground state. Slow dynamics of this ground state is observed around zero-dc field but above 3.4 T, zero-field excited spin states become the lowest in energy giving rise to the second hysteresis loop.

Among the cyanide-based SMMs, the $\{\text{Re}^{\text{IV}}\text{Mn}^{\text{II}}_4\}$ complex (**14**; $[(\text{PY5Me}_2)_4\text{Mn}_4\text{Re}(\text{CN})_7](\text{PF}_6)_5\cdot 6\text{H}_2\text{O}$; PY5Me₂ = 2,6-bis(1,1-bis(2-pyridyl)ethyl)-pyridine) based on the pentagonal bipyramidal $[\text{Re}^{\text{IV}}(\text{CN})_7]^{3-}$ module stands apart with a large barrier of 47 K ($\tau_0 = 2.4 \times 10^{-8}$ s).^{142,143} This system, depicted in Fig. 3, incorporates bulky $[(\text{PY5Me}_2)\text{Mn}^{\text{II}}]^{2+}$ units (Scheme 1o), which limit the nuclearity of the complex. At first look, the presence of an SMM behaviour in **14** seems surprising as the magnetic anisotropy of Mn^{II} is well-known to be very weak and ZFS is obviously meaningless for *S* = 1/2 systems like $[\text{Re}^{\text{IV}}(\text{CN})_7]^{3-}$. Indeed, the $(\text{NBu}_4)_3[\text{Re}(\text{CN})_7]$ precursor exhibits a strongly anisotropic *g* tensor with $g_{\parallel} = 3.66$ and $g_{\perp} = 1.59$ (from X-band EPR) reflecting the unquenched orbital angular momentum of the $^2\text{E}_1''(\text{d}^3)$ ground state in the idealized $D_{5\text{h}}$ symmetry.¹⁴⁴ Therefore the strong magnetic anisotropy of **14** is likely due to anisotropic $\text{Re}^{\text{IV}}\text{-Mn}^{\text{II}}$ exchange interactions, which have been described for isoelectronic $[\text{Mo}(\text{CN})_7]^{4-}\text{-Mn}^{\text{II}}$ systems in the frame of the super-exchange theory.¹⁴⁵ Similar complexes with $\{\text{Ni}^{\text{II}}_4\text{Re}^{\text{IV}}\}$ (**15**; $[(\text{PY5Me}_2)_4\text{Ni}_4\text{Re}(\text{CN})_7](\text{PF}_6)_5$) and $\{\text{Cu}^{\text{II}}_4\text{Re}^{\text{IV}}\}$ (**16**; $[(\text{PY5Me}_2)_4\text{Cu}_4\text{Re}(\text{CN})_7](\text{PF}_6)_5$) cores also exhibit slow relaxation of the magnetization although with significantly reduced Δ_{eff} 's.¹⁴³ While $\Delta_{\text{eff}}/k_{\text{B}} = 24$ K and $\tau_0 = 1.4 \times 10^{-7}$ s for **15**, only a small frequency dependence of a non-zero $\chi''(T)$ with $\nu_{\text{ac}} \leq 1.5$ kHz was observed for **16** suggesting a much smaller Δ_{eff} .¹⁴³ The potentially interesting magnetic properties of the $[\text{Mo}(\text{CN})_7]^{4-}$ module incorporated into molecular systems have been studied by Dunbar, Wang and co-workers. The first complex incorporating this moiety was $[\text{Mn}(\text{LN}_5)(\text{H}_2\text{O})_2]_2\{[\text{Mo}(\text{CN})_7]_8[\text{Mn}(\text{LN}_5)]_{10}[\text{Mn}(\text{LN}_5)(\text{H}_2\text{O})_4]\}\cdot x\text{H}_2\text{O}$ (LN_5 = 2,13-dimethyl-3,6,9,12,18-pentaazabicyclo-[12.3.1]octadeca-1(18),2,12,14,16-pentaene). This $\{\text{Mn}^{\text{II}}_{14}\text{Mo}^{\text{III}}_8\}$ (**18**) complex exhibits a large spin ground state (*S_T* = 31), but instead of possessing SMM properties, it shows a 3D ferrimagnetic ordering at low

temperature.¹⁴⁶ Very recently, the same group reported on three trinuclear $\text{Mn}^{\text{II}}\text{L}\text{-}[\text{Mo}^{\text{III}}(\text{CN})_7]\text{-Mn}^{\text{II}}\text{L}$ complexes where L is a pentadentate ligand.¹⁴⁷ In particular, the quasi-linear $\text{Mn}^{\text{II}}\text{-NC-Mo}^{\text{III}}\text{-CN-Mn}^{\text{II}}$ complex, $[\text{Mn}(\text{L}_{\text{N}5\text{Me}})(\text{H}_2\text{O})]_2[\text{Mo}(\text{CN})_7]\cdot 6\text{H}_2\text{O}$ (**19**, $\text{L}_{\text{N}5\text{Me}} = 2,6\text{-bis}(3,6\text{-diazahept-2-ene-2-yl})\text{pyridine}$, Fig. 4d), exhibits clear SMM properties with $\Delta_{\text{eff}}/k_{\text{B}} = 58.5(4)$ K and $\tau_0 = 2.0(3) \times 10^{-8}$ s. These characteristics make this complex the current record holder in terms of Δ_{eff} for cyanide-based SMMs. Additionally, this system exhibits a large *M* vs. *H* hysteresis loop at low temperatures with a coercive field of 2.0 T (with a 0.05 T s⁻¹ sweeping rate) at 1.8 K. Octacyanidometallates are known for $\text{W}^{\text{IV}/\text{V}}$, $\text{Mo}^{\text{IV}/\text{V}}$, $\text{Nb}^{\text{III}/\text{IV}}$ and Re^{V} metal ions. The incorporation of these units into coordination networks and their resulting magnetic properties have been the topics of reviews by Sieklucka and co-workers.^{148–151} Using these octacyanidometallate building blocks, Dunbar and co-workers isolated TBP complexes similar to the ones described earlier (2, Fig. 3, left), $[\text{Ni}^{\text{II}}(\text{tmphen})_2]_3[\text{W}^{\text{V}}(\text{CN})_2]$ (**20**), but no *M* vs. *H* hysteresis loop was observed down to 40 mK.¹⁵² Only a few reports on SMMs based on $[\text{M}^{\text{V}}(\text{CN})_8]^{3-}$ building blocks ($\text{M}^{\text{V}} = \text{Mo}^{\text{V}}$, W^{V} , Re^{V} (*S* = 0)) have been reported. These include large polynuclear complexes with stoichiometries such as $\{\text{Ni}^{\text{II}}_9\text{Mo}^{\text{V}}_6\}$ (**21**, *S_T* = 12; $[\text{Ni}\{\text{Ni}(\text{bpy})(\text{H}_2\text{O})_8\}\{\text{Mo}(\text{CN})_8\}_6]\cdot 12\text{H}_2\text{O}$),¹⁵³ $\{\text{Ni}^{\text{II}}_9\text{W}^{\text{V}}_6\}$ (**22**, *S_T* = 12; $[\text{Ni}\{\text{Ni}(\text{bpy})(\text{H}_2\text{O})_8\}\{\text{W}(\text{CN})_8\}_6]\cdot 23\text{H}_2\text{O}$,^{152,154}) and site-substituted Re^{V} analogues ($[\text{Co}_9(\text{CH}_3\text{OH})_{24}\{\text{W}(\text{CN})_8\}_5\{\text{Re}(\text{CN})_8\}\cdot x\text{CH}_3\text{OH}\cdot y\text{H}_2\text{O}$, **23**),¹⁵⁵ but only thin evidence of slow magnetic relaxation has been observed. Another family of heterometallic systems encompass mixed 3d–5d–4f species incorporating paramagnetic octacyanometallates,^{156–159} some of which exhibit SMM behaviour.^{159–161} Herein, the 3d–4f back-bone is based on bicompartimental Schiff-base ligands derived from *o*-vanillin and diamine ligands, which accommodate a Cu^{II} ion in a salen-type environment.^{162,163} With the phenolates and the methoxy groups, this unit constitutes a chelating metallo-ligand for lanthanide ions, which, subsequently, may coordinate the octacyanometallate by either the Cu^{II} or the Ln^{III} ion.

Heteroleptic cyanidometallates

Detailed reviews of the use of di- and tri-cyanidometallate precursors in the design of polynuclear systems have recently been published by Wang *et al.*^{164,165} Using these modules, the first indications of SMM behaviour in a cyanide-bridged system was found in a $\{\text{Mo}^{\text{III}}_6\text{Mn}^{\text{II}}\}$ complex (**24**; $\text{K}[(\text{Me}_3\text{tacn})_6\text{MnMo}_6(\text{CN})_{18}]\cdot (\text{ClO}_4)_3$; $\text{Me}_3\text{tacn} = N,N',N''\text{-trimethyl-1,4,7-triazacyclononane}$) complex incorporating *fac*- $[\text{Mo}^{\text{III}}(\text{Me}_3\text{tacn})(\text{CN})_3]$ units.¹⁶⁶ Each of these modules coordinates through only one cyanide ligand to the central Mn^{II} ion leading to an approximately prismatic structure (Fig. 6). The intra-complex $\text{Mo}^{\text{III}}\text{-Mn}^{\text{II}}$ antiferromagnetic interactions ($J_{\text{Mo-Mn}}/k_{\text{B}} = -9.6$ K) yield an *S_T* = 13/2 spin ground state. Fitting of the *M* vs. *H/T* data revealed an Ising-type magnetic anisotropy of $D/k_{\text{B}} = -0.47$ K.

Notably, the isostructural $\{\text{Cr}^{\text{III}}_6\text{Mn}^{\text{II}}\}$ (**25**; $\text{K}[(\text{Me}_3\text{tacn})_6\text{MnCr}_6(\text{CN})_{18}]\cdot (\text{ClO}_4)_3$) complex did not exhibit SMM properties,¹⁶⁷ likely due to a stronger magnetic anisotropy exhibited by the Mo^{III} unit over the Cr^{III} building block. For d³ ions (t_{2g}^3), like Mo^{III} , in an axially perturbed ligand field, the magnetic anisotropy is primarily induced by the mixing of the $^4\text{A}_{2g}(\text{O}_h)$ ground



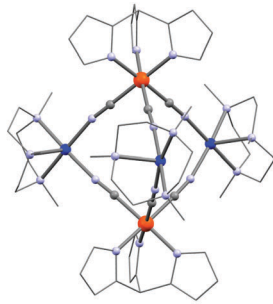
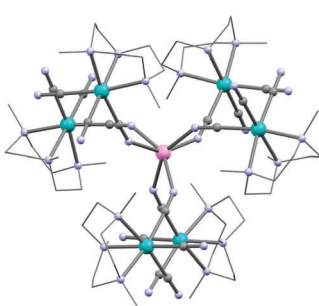


Fig. 6 Molecular structure of **24** (left) and **29** (right). Colour code: Mo, turquoise; Cu, maroon; Fe, orange; Mn, pink; N, pale blue; C, grey.

state with the excited ${}^4T_{2g}(O_h)$ state *via* spin-orbit coupling.¹⁶⁸ If only this mixing is taken into account, the D parameter scales as ζ_{nl}^2 . For $3d^3$ metal ion such as V^{2+} , Cr^{3+} and Mn^{4+} for which the spin-orbit coupling is relatively weak, this second-order contribution to the magnetic anisotropy is often negligible, whereas this effect becomes important for $4d$ and $5d$ transition metal ions.

The *trans*-[ReCl₄(CN)₂]²⁻ building block reported by Long and co-workers is another interesting example of a heteroleptic cyanide-based 5d metal ion module.¹⁶⁹ This building block is unique in the sense of being the sole example of a paramagnetic mixed halide-cyanide complex. In addition, it offers both strong magnetic anisotropy as well as effective mediation of super-exchange.^{170,171} The latter property is well illustrated in the [NBu₄][TpCuReCl₄(CN)₂]·1.33CH₃CN chain system (**26**, Tp⁻ = hydrotris(pyrazol-1-yl)borate) exhibiting the strongest ferromagnetic interaction mediated by a cyanide bridge ($J_{Cu-Re}/k_B = 41$ K) reported until now.⁹⁶ Remarkably, the Cu^{II} JT axis in **26** is not placed along the Cu-NC axes and the short Cu-N bond lengths facilitate the pronounced interaction. The reaction of *trans*-[ReCl₄(CN)₂]²⁻ with [(TPA^{2C(O)NHtBu})-Fe^{II}(CF₃SO₃)]⁺ (TPA^{2C(O)NHtBu} = 6,6'-(pyridin-2-ylmethylazanediy)-bis(methylene)bis(*N*-*tert*-butylpicolinamide)) affords a dinuclear cyanido-bridged SMM (**27**; (TPA^{2C(O)NHtBu})₂FeReCl₄(CN)₂).¹⁷² The pentagonal bipyramidal Fe^{II} precursor ($S = 2$) has (as the triflate complex) a strong magnetic anisotropy reflected by its ZFS parameters: $D/k_B = 11$ K and $|E|/k_B = 3.2$ K. ac susceptibility measurements reveal only an increase of $\chi''(\nu_{ac})$ without a maximum (with $\nu_{ac} \leq 1.5$ kHz) indicating a small Δ_{eff} . Despite the promising Fe^{II}-Re^{IV} ferromagnetic interactions and the strong magnetic anisotropy of the building blocks, the non-collinearity of anisotropy tensors might be responsible for the small overall anisotropy of the final complex emphasizing the necessity to control the geometry of the designed polynuclear SMMs. Several other magnetic systems based on the *trans*-[ReCl₄(CN)₂]²⁻ module have been reported but most of them are chains (that are commonly observed for *trans*-dicyanidometallates) and SCM compounds.^{169,171} Only a few other similar building blocks based on 4d/5d metal ions are known including *trans*-[Ru^{III}(acac)₂(CN)₂]⁻ (acac = acetylacetone),¹⁷³ [M^{III}(salen)(CN)₂]⁻ (M = Ru,¹⁷⁴ Os¹⁷⁵), and *trans*-[Ru^{III}(8-quin)₂(CN)₂]⁻ (quin = 8-quinolinolato),¹⁷⁶ but none of them have been

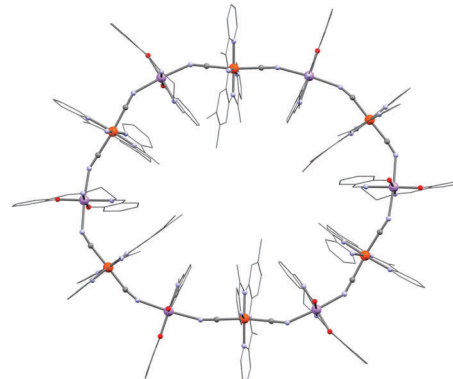


Fig. 7 Molecular structure of **28**. Colour code: Fe, orange; Mn, purple; O, red; N, pale blue; C, grey.

used to design SMMs yet. Returning to the first row transition metal ions, a particularly exotic complex is obtained with the *trans*-dicyanidometallate [Fe^{III}(bpmb)(CN)₂]⁻ module: [Mn^{III}(salen)]₆[Fe^{III}(bpmb)(CN)₂]₆·7H₂O (**28**, H₂bpmb = 1,2-bis(pyridine-2-carboxamido)-4-methylbenzene). Instead of forming a chain system, a twelve membered wheel is crystallized as shown in Fig. 7.^{177,178} As the magnetic anisotropy is dictated by the JT distorted Mn^{III} ions, the overall magnetic anisotropy of **28** is accordingly small leading to SMM properties with an effective energy barrier of only 7.5 K.

Several facial tricyanidoiron(III) complexes with the auxiliary ligand sphere occupied by various pyrazolylborate ligands, *fac*-[LFe^{III}(CN)₃]⁻, have been utilized as modules to synthesize SMMs.¹⁷⁹⁻¹⁸⁷ Most of these SMM systems encompass Ni^{II} ions and commonly give rise to square-based structures. However, the reaction of the simple [TpFe^{III}(CN)₃]⁻ module with [(Me₃tacn)-Cu^{II}(H₂O)₂](ClO₄)₂ affords a remarkable TBP complex (**29**, [Tp₂(Me₃tacn)₃Cu₃Fe₂(CN)₆](ClO₄)₄·2H₂O Fig. 6).¹⁷⁹ The apparent preference of the Cu^{II} ion to penta-coordinated geometry prevents the formation of a molecular square or cube structure as the Me₃tacn ligand blocks three facial coordination sites. The Cu^{II} ($S = 1/2$) and low-spin Fe^{III} ($S = 1/2$) magnetic centres couple ferromagnetically ($J_{Cu-Fe}/k_B = 12$ K) stabilizing an $S_T = 5/2$ ground state that combined with a relatively strong magnetic anisotropy ($D/k_B = -8.2$ K obtained from fitting of reduced magnetization data) induces SMM properties with $\Delta_{eff}/k_B = 23$ K ($\tau_0 = 4.8 \times 10^{-8}$ s). As the local spins are all $S = 1/2$, the magnetic anisotropy is likely the result of the orbital angular momentum of the low-spin Fe^{III} modules. A structural analogue is obtained when [TpFe^{III}(CN)₃]⁻ is reacted with [Ni^{II}(cyclen)](BF₄)₂ (cyclen = 1,4,7,10-tetraazacyclododecane) giving a {Fe^{III}₂Ni^{II}₃} SMM (**30**; [(cyclen)Ni]₃[TpFe(CN)₃]₂(BF₄)₄·4H₂O). The TBP geometry is induced by the *cis* configuration of the accessible coordination sites of the Ni^{II} building block imposed by the small cavity of the cyclen ligand.¹⁸⁸ This complex displays intra-molecular ferromagnetic interactions ($J_{Ni-Fe}/k_B = +7.8$ K, $S_T = 4$) and shows the onset of $\chi''(T)$ peaks above 1.8 K suggesting SMM properties.

Other *fac*-tricyanido building blocks such as [Re^{II}(triphos)(CN)₃]⁻ (triphos = 1,1,1-tris(diphenylphosphinomethyl)ethane) have been studied by Dunbar and co-workers who have reported a {Mn^{II}₄Re^{II}₄}

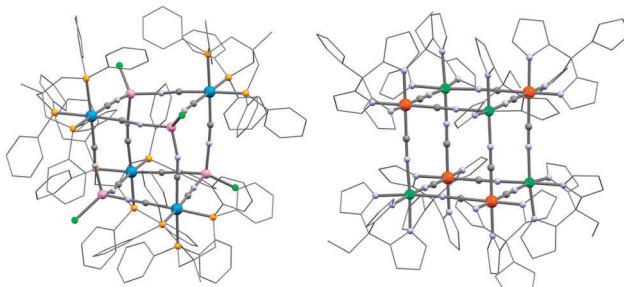


Fig. 8 Molecular structures of **31** (left) and **33** (right) cubes. Colour codes: Re, maroon; Ni, turquoise; Fe, orange; Mn, pink; Cl, green; P, yellow; N, pale blue; C, grey.

(**31**; $[\text{MnCl}]_4[\text{Re}(\text{triphos})(\text{CN})_3]_4$) SMM^{189,190} and polymeric systems¹⁹¹ based on this module. The structure of the parent complex, **31**, is a molecular cube as depicted in Fig. 8. Other divalent metal ions such as Fe^{II} , Co^{II} , Ni^{II} and Zn^{II} have been incorporated into analogous systems, but only the Mn^{II} complex was shown to be an SMM ($\Delta_{\text{eff}}/k_{\text{B}} = 13 \text{ K}$, $\tau_0 = 3.25 \times 10^{-7} \text{ s}$).¹⁹² The static magnetic properties are dominated by the antiferromagnetic interactions between Re^{II} ($S = 1/2$) and Mn^{II} ($S = 5/2$) spins but a detailed analysis of the experimental magnetic data becomes highly complicated due to orbital contributions to the magnetic exchange mechanism and a large temperature independent paramagnetism (TIP) of the Re^{II} ion.¹⁹³

Glaser and co-workers extended their strategy of molecular recognition with triple-salen ligands by exchanging $[\text{Cr}(\text{CN})_6]^{3-}$ with *fac*- $[\text{Cr}^{\text{III}}(\text{Me}_3\text{tacn})(\text{CN})_3]$. The three (*fac*) positions occupied by the Me_3tacn ligand around the Cr^{III} ion force the *fac*- $[\text{Cr}^{\text{III}}(\text{Me}_3\text{tacn})(\text{CN})_3]$ module to coordinate only one $\{\text{Mn}^{\text{III}}_3\}$ triple-salen moiety (**32**; $[(\text{talen}^{\text{tBu}})(\text{Mn}(\text{MeOH}))_3][(\text{Me}_3\text{tacn})\text{Cr}(\text{CN})_3]\text{[ClO}_4\text{]}_3$).¹⁹⁴ For this system, the $\chi''(T)$ data only show weakly frequency-dependent onsets of peaks between 1.8 and 2.5 K suggesting a lower spin-relaxation barrier than in the $\{\text{Mn}^{\text{III}}_6\text{Cr}^{\text{III}}\}$ complex (**12**, $\Delta_{\text{eff}}/k_{\text{B}} = 25.4 \text{ K}$) as expected when lowering the spin ground state from $S_{\text{T}} = 21/2$ (**12**) to $7/2$ (**32**).

The groups of Holmes, Oshio and Zuo reported $\{\text{Fe}^{\text{III}}_4\text{Ni}^{\text{II}}_4\}$ molecular cubes exhibiting SMM properties.¹⁹⁵⁻¹⁹⁹ All the reported examples are based on cyanido-based Fe^{III} modules with tris(pyrazol-1-yl)borate capping ligand derivatives, whereas a plethora of ligands, primarily amines, have been employed for the more labile Ni^{II} moiety. The prototypical example, $\{[(\text{pzTp})\text{Fe}(\text{CN})_3]_4[\text{Ni}(\text{tpe})]_4\}[\text{OTf}]_4\text{-10DMF-}2\text{Et}_2\text{O}$, (**33**, Fig. 8) reported by Holmes and co-workers involves the $[(\text{pzTp})\text{Fe}^{\text{III}}(\text{CN})_3]^-$ building block (pzTp^- = tetra(pyrazol-1-yl)borate; OTf^- = trifluoromethanesulfonate) and a Ni^{II} site with a 2,2,2-tris(pyrazolyl)ethanol (tpe) capping ligand.¹⁹⁶ The $\text{Fe}^{\text{III}}-\text{Ni}^{\text{II}}$ ferromagnetic coupling ($J/k_{\text{B}} = +9.5(5) \text{ K}$) yields an $S_{\text{T}} = 6$ ground state as found for the other analogues.¹⁹⁵⁻¹⁹⁹ Fitting of the M vs. H/T data allowed an estimation of D/k_{B} at about -0.33 K (and thus $\Delta_{\text{eff}}/k_{\text{B}} = |D|S_{\text{T}}^2 \approx 12 \text{ K}$) that corroborates the experimental finding of only a small Δ_{eff} . It is worth mentioning that a similar $\{\text{Fe}^{\text{III}}_4\text{Ni}^{\text{II}}_4\}$ complex (**34**; $[(\text{tach})_4(\text{H}_2\text{O})_{12}\text{Ni}_4\text{Fe}_4(\text{CN})_{12}]\text{Br}_8\text{-}18\text{H}_2\text{O}$) based on the tach (1,3,5-triaminocyclohexane) capping ligand was synthesized by Long and co-workers but no slow relaxation of magnetization

was reported.²⁰⁰ Recently, Oshio and co-workers reported a mixed-valence cube complex $\text{Na}[(\text{Tp})_4\text{Fe}^{\text{III}}_2\text{Fe}^{\text{II}}_2(\text{CN})_{12}\text{Ni}^{\text{II}}_4(\text{L})_4](\text{BF}_4)_3$ (**35**) incorporating a redox-active ligand: $\text{L} = \alpha\text{-}(\text{4}'\text{-methyl-4,5-dimethylthio-tetrathiafulvalene-5'-thio})\text{-}\alpha\text{-[tris-2,2,2-(1-pyrazolyl)-ethoxy]-}p\text{-xylene}$. Unfortunately this complex, which was not structurally characterized, only exhibits a small frequency-dependent increase of the $\chi''(T)$ data between 1.8 and 3 K.¹⁹⁹ An analogous $\{\text{Fe}_4\text{Co}_4\}$ cube complex, $\{[(\text{pzTp})\text{Fe}(\text{CN})_3]_4[\text{Co}(\text{tpe})]_4\}[\text{ClO}_4]_4\text{-13DMF-}4\text{H}_2\text{O}$ (**36**), was also reported but instead of exhibiting SMM properties, it displays temperature- and light-induced magnetic bistability²⁰¹ controlled by an intra-molecular electron transfer and two different redox configurations: *i.e.* the paramagnetic $\{\text{Fe}^{\text{III}}_4\text{Co}^{\text{II}}_4\}$ and diamagnetic $\{\text{Fe}^{\text{II}}_4\text{Co}^{\text{III}}_4\}$ states.

From a strategic point of view, the nearly cubic structure of the previously described SMMs does not appear to be the ideal geometry to obtain SMM properties (due to a near compensation of magnetic anisotropy tensors). Therefore, researchers have been trying to reduce the $\{\text{Fe}^{\text{III}}_4\text{Ni}^{\text{II}}_4\}$ cubes into less-symmetrical smaller fragments like defect cubanes, squares and trinuclear complexes. Interestingly, the use of facial tri-cyanido modules also stabilizes molecular square SMMs with alternating Fe^{III} and Ni^{II} ,^{181,182,184,202-205} or Cu^{II} metal ions.²⁰⁶ In these $\text{Fe}^{\text{III}}\text{-}\text{Ni}^{\text{II}}$ systems illustrated by $[\text{Tp}^*\text{Fe}(\text{CN})_3]_2\text{-}[\text{Ni}(\text{DMF})_4]_2(\text{OTf})_2\text{-}2\text{DMF}$ (**37**) in Fig. 9 (Tp^* = hydridotris-(3,5-dimethylpyrazol-1-yl)borate),¹⁸¹ the $\text{Fe}^{\text{III}}\text{-}\text{Ni}^{\text{II}}$ interaction is ferromagnetic with $J_{\text{Ni-Fe}}$ coupling constants up to $+10.1 \text{ K}$,¹⁸⁴ giving rise to an $S_{\text{T}} = 3$ ground state. It was argued that the distortion of the Ni^{II} coordination sphere does not significantly alter the SMM properties suggesting that orbital contributions from the $S = 1/2$ Fe^{III} module is the main origin of the SMM properties in these molecular $\text{Fe}^{\text{III}}\text{-}\text{Ni}^{\text{II}}$ squares.²⁰⁷ Their effective

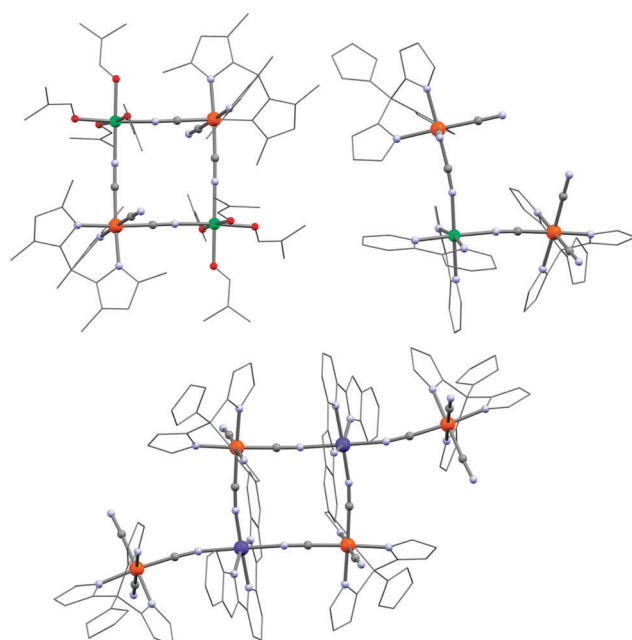


Fig. 9 Molecular structures of **37** (top, left), **38** (top, right) and **42** (bottom, in the $\{\text{Fe}^{\text{II}}_2\text{Co}^{\text{III}}_2\text{Fe}^{\text{II}}_2\}$ state obtained at $T = 100 \text{ K}$). Colour codes: Ni, turquoise; Co, purple; Fe, orange; O, red; N, pale blue; C, grey.



SMM energy gaps are relatively moderate with the largest reported value being $\Delta_{\text{eff}}/k_{\text{B}} = 29.0(4)$ K.²⁰²

Defect square $\{\text{Fe}^{\text{III}}_2\text{Ni}^{\text{II}}\}$ SMMs were also obtained, for example by reaction of $(\text{NET}_4)[(\text{pzTp})\text{Fe}^{\text{III}}(\text{CN})_3]$ with Ni^{II} and bpy (38, $\{[(\text{pzTp})\text{Fe}(\text{CN})_3]_2[\text{Ni}(\text{bpy})_2]\} \cdot 2\text{H}_2\text{O}$; bpy = 2,2'-bipyridine).¹⁸³ Interestingly, this complex shown in Fig. 9 exhibits a clear SMM signature by ac susceptibility measurements despite the small $S_{\text{T}} = 2$ ground state induced by the intra-complex ferromagnetic interactions ($J_{\text{Fe-Ni}}/k_{\text{B}} = 7.0(2)$ K). In the absence of a static dc field, the energy barrier is about 12.0 K ($\tau_0 = 4 \times 10^{-7}$ s) that increases up to 20.6 K ($\tau_0 = 2 \times 10^{-8}$ s) in a small dc field (2000 Oe). Such trinuclear SMMs can themselves be viewed as building-blocks for larger molecular $\{\text{Fe}^{\text{III}}_2\text{Ni}^{\text{II}}\}_n$ structures where $n = 2$ or 3. Although not synthetically assembled from pre-isolated trinuclear precursors, an *exo*-cyclic $\{\text{Fe}^{\text{III}}_4\text{Ni}^{\text{II}}_2\}$ SMM (39; $\{[(\text{Tp}^{\text{*Me}})\text{Fe}(\text{CN})_3]_4[\text{Ni}(\text{DMF})_3]_2\} \cdot 4\text{DMF} \cdot 2\text{H}_2\text{O}$; $\text{Tp}^{\text{*Me}} = \text{tris}(3,4,5\text{-trimethylpyrazole})\text{borate}$) and a *fused* system of *exo*-cyclic squares $\{\text{Fe}^{\text{III}}_6\text{Ni}^{\text{II}}_3\}$ (40; $\{[(\text{Tp}^{\text{*Me}})\text{Fe}(\text{CN})_3]_6[\text{Ni}(\text{MeOH})_3]_2[\text{Ni}(\text{MeOH})_2]\} \cdot 3\text{H}_2\text{O} \cdot 8\text{MeOH}$) have been reported.²⁰⁸ In these two complexes, the Ni^{II} sites connect three $\{[(\text{Tp}^{\text{*Me}})\text{Fe}(\text{CN})_3]\}^-$ modules. Their remaining positions are occupied by rather labile solvent molecules, which do not apply any particular geometrical constraints on the coordination sphere. The energy barriers for these $\{\text{Fe}^{\text{III}}_2\text{Ni}^{\text{II}}\}_n$ SMMs are slightly higher than for the trinuclear parent complex, 38, with $\Delta_{\text{eff}}/k_{\text{B}} = 15.6$ K and 17.7 K in zero-dc field and 26 K and 24.5 K in 1500 and 600 Oe for 39 and 40, respectively.

The use of the same Fe^{III} module, $\{[(\text{Tp}^{\text{*Me}})\text{Fe}^{\text{III}}(\text{CN})_3]\}^-$, and geometrically constraining the Ni^{II} coordination sphere by the tetradeinate tren ligand (tren = tris(2-aminoethyl)amine), leaving only two *cis*-positions accessible, leads to an octanuclear $\{\text{Fe}^{\text{III}}_4\text{Ni}^{\text{II}}_4\}$ complex (41; $\{[(\text{Tp}^{\text{*Me}})\text{Fe}(\text{CN})_3]_4[\text{Ni}(\text{tren})]_4[\text{ClO}_4]_4\} \cdot 7\text{H}_2\text{O} \cdot 4\text{MeCN}$).¹⁸⁵ Its complicated molecular structure can be viewed as an “unwrapped” version of the $\{\text{Fe}^{\text{III}}_4\text{Ni}^{\text{II}}_4\}$ cube. This low-symmetric complex exhibits one of the largest effective energy barriers (33 K) for any cyanide-based 1st row transition metal SMM.

As previously mentioned for a $\{\text{Fe}_4\text{Co}_4\}$ cube complex,²⁰¹ a few examples of molecular $\{\text{Fe}^{\text{III/II}}_2\text{Co}^{\text{II/III}}_2\}$ squares have been reported^{209–215} to exhibit photo- and thermally-assisted intra-molecular charge transfer similar to the effect observed in three-dimensional Fe/Co Prussian Blue analogues.⁹⁷ The principle of this phenomenon is based on the reversible interconversion of diamagnetic $\{\text{Fe}^{\text{II}}_{\text{LS}}(\mu\text{-CN})\text{Co}^{\text{III}}_{\text{LS}}\}$ pairs into paramagnetic $\{\text{Fe}^{\text{III}}_{\text{LS}}(\mu\text{-CN})\text{Co}^{\text{II}}_{\text{HS}}\}$ pairs by light irradiation and thermal energy. Very recently, SMM properties in a photo-induced state were observed for the first time in the hexanuclear complex, $\{[(\text{pzTp})_4\text{Fe}_4(\text{CN})_6(\mu\text{-CN})_6\text{Co}_2(\text{bimpy})_2]\} \cdot 2^n\text{PrOH} \cdot 4\text{H}_2\text{O}$ ²¹⁶ (42; bimpy = 2,6-bis(benzimidazol-2-yl)pyridine) shown in Fig. 9. The use of the tridentate bimpy ligand permits only three vacant sites on the Co metal ions in a *mer*-position allowing the central $\{\text{Fe}^{\text{III/II}}_2\text{Co}^{\text{II/III}}_2\}$ square to be decorated by two $\{[(\text{pzTp})\text{Fe}^{\text{III}}(\mu\text{-CN})(\text{CN})_2]\}^-$ units. These *exo*-cyclic moieties are permanently in a LS (t_{2g}^5) state, whereas the $\{\text{Fe}_2\text{Co}_2\}$ square consists of (i) HS Co^{II} ($S = 3/2$) and LS Fe^{III} ($S = 1/2$) metal ions above 250 K and (ii) LS Co^{III} ($S = 0$) and LS Fe^{II} ($S = 0$) sites below 200 K,

as evidenced from the χT vs. T data and single-crystal X-ray crystallography at different temperatures. Upon an 808 nm irradiation at 5 K, the χT product increases to $20.3 \text{ cm}^3 \text{ K mol}^{-1}$ as a result of an intra-square electron transfer from a diamagnetic central $\{\text{Co}^{\text{III}}_2\text{Fe}^{\text{II}}_2\}$ core to an exchange-coupled $\{\text{Co}^{\text{II}}_2\text{Fe}^{\text{III}}_2\}$ unit. Before irradiation, ac susceptibility measurements did not detect any sign of slow relaxation of magnetization in 42, but in its photo-excited state, clear frequency-dependent $\chi''(T)$ peaks were observed, suggesting that this complex was the first photo-switchable SMM. The associated spin-reversal barrier was estimated at about 26 K in a static field of 500 Oe.

In contrast to the *fac*-tricyanido systems, *mer*-tricyanido modules have received much less attention.^{217–222} *mer*-Tricyanide complexes are well-known especially for iron(III) as illustrated by the $[\text{Fe}^{\text{III}}(\text{bpc})\text{(CN)}_3]^-$ (bpc = bis(2-pyridylcarbonyl)amine),²²³ and $[\text{Fe}^{\text{III}}(\text{pcq})\text{(CN)}_3]^-$ (pcq = 8-(pyridine-2-carboxamido)quinoline) building blocks.^{217,224} As for the *trans*-dicyanido modules (*vide supra*), these units are favoring one-dimensional assembly unless steric constraints from the other building blocks impose otherwise. To the best of our knowledge, no SMMs incorporating these *mer*-tricyanido building blocks have been reported so far.

4. Non-cyanide based precursors

Undoubtedly, cyanide remains the coordination chemist's favourite bridging ligand in the quest for new SMMs and functional materials. The cyanide-based complexes often possess three essential properties: (i) integrity in solution, (ii) relatively linear bridging modes between metal ions (Fig. 2) and (iii) a redox-activity that does not alter the complex structure. None of these properties are indeed exclusive to the cyanide-based building blocks, and magnetic modules based on other type of bridging groups should be considered in the design of SMM systems.

Halide and *pseudo*-halide based modules

Although a few examples of SMMs with chloride bridges have been reported,²²⁵ no examples assembled from modules can be said to exist. Building-block examples based on *pseudo*halides (other than cyanides) including azide and (iso)thiocyanate are also extremely rare^{226,227} and no examples of SMMs synthesized by a modular approach have been reported. Gao, Lau and co-workers reported the *mer*- $[\text{Ru}^{\text{III}}(\text{sap})(\text{N}_3)_3]^-$ module (H₂sap = *N*-salicylidene-*o*-aminophenol) but its reaction with Ni^{II} or Co^{II} afforded polynuclear complexes incorporating diamagnetic Ru^{VI} ions.²²⁸ Isoelectronic three-atom ligands such as cyanate, thiocyanate or azide have been used to prepare complexes of paramagnetic transition metal ions but no SMM systems incorporating these modules have been prepared so far. Remarkably, relatively strong exchange interactions have been observed in $\text{Ni}^{\text{II}}\text{-SCN-Cr}^{\text{III}}$ and $\text{Ni}^{\text{II}}\text{-SCN-Mo}^{\text{III}}$ linkages but SMMs incorporating such units have not been reported.²²⁶

At this stage of this Feature article, it is natural to wonder if the modular approach can use a single atom as a magnetic bridge to design SMMs. An obvious choice would be oxide or hydroxide based building blocks but they are not easy to



employ due to the strong basicity of most paramagnetic complexes. In principle, a reasonable approach could involve complexes with metal ions in a high oxidation state, which should have less basic oxide, or, eventually, nitride complexes. Only two examples of SMMs incorporating oxide-based modules have been reported, but both involve diamagnetic Re^{V} metal ions.^{229,230} Building blocks based on fluoride as the potential bridging ligand to synthesize magnetic materials are also largely unexplored.^{231–236} Being isoelectronic to oxide, the incorporation of fluoride is not obvious. In addition to its basicity, the oxide group has the tendency to form non-linear bridges (Fig. 2) between two or more metal ions making it less appealing as the bridging ligand. These two effects appear less pronounced for fluoride. Several mononuclear 3d metal ion fluoride complexes are known and commonly fluoride leads to linear or almost linear bridges.²³⁷ The main synthetic problem of these fluoride complexes arises from the inherent lability of many fluoride complexes. However, this issue can be overcome by using, for instance, kinetically robust Cr^{III} fluoride complexes,²³² or by enforcing robustness with selected auxiliary ligands as discussed earlier. Being a “hard” ligand, fluoride has a strong preference for “hard” metal ions such as lanthanides. Further discussions about the controlled design of 3d–4f SMM systems with fluoride-based modules will be presented in the last paragraph of this section dedicated to lanthanide and actinide based building-blocks. We recently reported $(\text{PPh}_4)_2[\text{ReF}_6]\cdot 2\text{H}_2\text{O}$ (43) incorporating a close-to-octahedral $[\text{ReF}_6]^{2-}$ anion to exhibit slow relaxation of the magnetization.⁶⁰ This interesting module in 43 has a large zero-field splitting of $D/k_{\text{B}} = +34.0$ K and $|E|/k_{\text{B}} = 3.7$ K as determined from inelastic neutron scattering and high-field EPR spectroscopy.⁶⁰ The strong magnetic anisotropy combined with the ability to bridge several metal centres make homoleptic fluoride-complexes, such as $[\text{ReF}_6]^{2-}$, interesting, but completely unexplored modules for SMMs.

Oxalate-based modules

Trisoxalatometallate(III)s, $[\text{M}(\text{ox})_3]^{3-}$, have been widely employed for assembling magnetic materials.²³⁸ This interest is motivated by the strong preference of the oxalate group to bridge two metal ions in a double-chelate fashion. However, the propensity of the $[\text{M}(\text{ox})_3]^{3-}$ unit to form extended systems makes these precursors less suitable to design SMMs, unless sterical constraints imposed by capping ligands are introduced on the acceptor metal ions. This problem can also be overcome by turning to heteroleptic oxalate systems with an appropriate choice of capping ligands. For instance, an interesting Re^{IV} module, $[\text{Re}^{\text{IV}}\text{Cl}_4(\text{ox})]^{2-}$, has been reported.²³⁹ The d^3 -configuration of the Re^{IV} ion gives a kinetically robust and hydrolytically stable building block. In combination with Ni^{II} metal ions, a propeller-shaped $\{\text{Ni}^{\text{II}}\text{Re}^{\text{IV}}_3\}$ complex ($(\text{NBu}_4)_4[\text{Ni}(\text{ReCl}_4(\text{ox}))_3]$, 44; Fig. 10) is formed.^{240,241} Modelling of the χT vs. T data gave a ferromagnetic Ni^{II} –ox– Re^{IV} interaction ($J_{\text{Re-Ni}}/k_{\text{B}}$) of +12 K. It is interesting to note that the field dependence of the magnetization for the $(\text{PPh}_4)_2[\text{ReCl}_4(\text{ox})]$ precursor reveals a strong magnetic anisotropy that has been estimated at $D/k_{\text{B}} \approx 86$ K.²³⁹ Notably, Martínez-Lillo *et al.* recently reported NBu_4^+ salts of

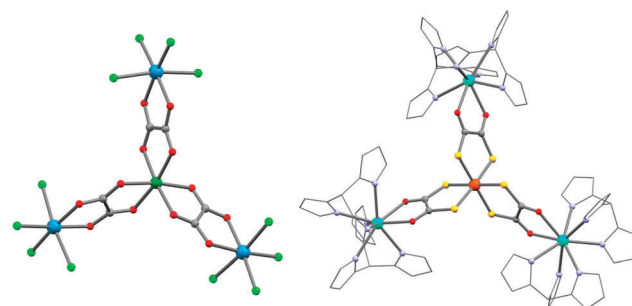


Fig. 10 Molecular structures of 44 (left) and 56 (right). Colour codes: Dy, turquoise; Re, marine; Ni, dark green; Fe, orange; Cl, light green; S, yellow; O, red; N, light blue; C, grey.

$[\text{ReCl}_4(\text{ox})]^{2-}$ and $[\text{ReBr}_4(\text{ox})]^{2-}$, to display SMM properties in small dc fields.²⁴² For 44, an out-of-phase χ'' signal was clearly visible in zero dc field, but under 2000 Oe, the spin-relaxation slows down as expected in presence of significant QTM. In a recent communication, the same authors reported a $\{\text{Gd}^{\text{III}}\text{Re}^{\text{IV}}_4\}$ four-bladed propeller ($(\text{NBu}_4)_4[\text{Gd}(\text{ReBr}_4(\mu\text{-ox}))_4(\text{H}_2\text{O})]\cdot \text{H}_2\text{O}$), but no slow relaxation of the magnetization was observed.²⁴³ So far, the only example of SMM behaviour in a 3d transition metal oxalate complex is $\{[\text{Cr}^{\text{III}}(\text{bpy})(\text{ox})_2]_2\text{Co}^{\text{II}}(\text{Me}_2\text{phen})\}\cdot 4\text{H}_2\text{O}$ (45; $\text{Me}_2\text{phen} = 2,9\text{-dimethyl-1,10-phenanthroline}$) that is obtained by the reaction of the $[\text{Cr}^{\text{III}}(\text{bpy})(\text{ox})_2]^-$ module with Co^{II} in the presence of the Me_2phen ligand. Only an onset of $\chi''(T)$ peaks is observed above 1.8 K, suggesting SMM properties and a small energy barrier.²⁴⁴

Acceptor modules

Some of the most commonly used modules to design SMMs are acceptor type units made of a Mn^{III} ion and a Schiff base (SB) ligand (see *e.g.* Scheme 1j). Polynuclear complexes based on these Schiff base complexes (abbreviated $\{\text{Mn}(\text{SB})\}^+$) have been reviewed by Miyasaka *et al.*¹²⁰ and along this Feature article we have already shown several examples of SMMs incorporating these units (Fig. 4, 5 and 7). The Schiff base ligands are often tetradentate to the Mn^{III} site occupying equatorial positions and allowing the two remaining apical positions to be accessible for further coordination for example with a cyanide group.^{88,116–119,121–123} The $\{\text{Mn}(\text{SB})\}^+$ units constitute a class of very useful modules for SMM synthesis due to their relatively strong magnetic anisotropy reflected in a large negative value of D estimated up to -6 K.^{124,245} In solution, the mononuclear $\{\text{Mn}(\text{SB})\}^+$ unit is in equilibrium with an “out-of-plane” dinuclear form (see Scheme 1k) in which the phenolate oxygens bridge two $\{\text{Mn}(\text{SB})\}^+$ moieties along the JT axes.¹²⁰ Depending on the structural parameters, the $\text{Mn}^{\text{III}}\text{–Mn}^{\text{III}}$ interaction through the bis-phenolate oxygens in this dinuclear module is often ferromagnetic in nature due to an accidental orthogonality of the d_{z^2} orbital occupied by one electron and the empty $d_{x^2-y^2}$ orbital of the other Mn^{III} centre. Due to this ferromagnetic interaction, that leads to an $S_{\text{T}} = 4$ spin ground state, and the coaxial ZFS Mn^{III} tensors, the $[\text{Mn}^{\text{III}}_2(\text{saltmen})_2(\text{ReO}_4)_2]$ complex (46; saltmen $^{2-} = \text{N},\text{N}'\text{-}(1,1,2,2\text{-tetramethylene})\text{bis}(\text{salicylidene-iminate})$) was found to be an SMM (Fig. 1).⁶¹ Since then,



several other $\{\text{Mn}_2(\text{SB})_2\}^{2+}$ SMMs have been reported.^{246,247} These out-of-plane $\{\text{Mn}_2(\text{SB})_2\}^{2+}$ building blocks have also been employed extensively to obtain photomagnetic chains,²⁴⁸ SCMs^{84,87–89} and two-dimensional networks by assembly with appropriate modules.^{22,249–252}

The terminal labile positions of the $\{\text{Mn}^{\text{III}}_2(\text{SB})_2\}^{2+}$ module can be decorated by other building blocks, for instance the $S = 1/2$ $[\text{W}^{\text{V}}(\text{CN})_6(\text{bpy})]^-$ unit yielding a $\{\text{Mn}^{\text{III}}_2\text{W}^{\text{V}}_2\}$ linear complex $[(\text{W}(\text{bpy})(\text{CN})_6)_2[\text{Mn}(\text{L})_2]_2 \cdot 3\text{H}_2\text{O}$ with $\text{L} = N,N'$ -bis(2-hydroxyacetophenylidene)-1,2-diaminopropane, **47**; Fig. 11).²⁵³ Overall, **47** is ferromagnetically coupled, $J_{\text{W}-\text{Mn}}/k_{\text{B}} = +1.2$ K and $J_{\text{Mn}-\text{Mn}}/k_{\text{B}} = +1.4$ K, leading to an $S_{\text{T}} = 5$ ground state. Although the energy barrier of 32 K is relatively large, the τ_0 pre-exponential factor is small, 5.1×10^{-12} s, and thus the relaxation of the magnetization is observed using the ac technique only below 3 K.

Other building blocks such as aldoximates have been also associated with $\{\text{Mn}^{\text{III}}_2(\text{SB})_2\}^{2+}$ moieties as exemplified by the series of tetranuclear $[\text{Mn}^{\text{III}}(5\text{-Rsaltmen})\text{Ni}^{\text{II}}(\text{pao})(\text{bpy})_2]_2(\text{ClO}_4)_4$ complexes (**48**; pao = pyridine-2-aldoximate) where R can be H, Cl, Br or OMe.²⁵⁴ The relatively strong antiferromagnetic $\text{Mn}^{\text{III}}-\text{Ni}^{\text{II}}$ interactions ($-26 \text{ K} < J_{\text{Mn}-\text{Ni}}/k_{\text{B}} < -24 \text{ K}$ depending on the system) leads to a relatively small $S_{\text{T}} = 2$ ground state for the complexes, which do not show any slow relaxation of the magnetization in zero-dc field above 1.8 K. However, two related trinuclear $\text{Ni}^{\text{II}}\text{-aldoximate}$ SMMs, $[\text{Mn}_2(5\text{-Rsaltmen})_2\text{Ni}(\text{pao})_2(\text{phen})](\text{ClO}_4)_2$ (R = Cl (**49**), Br (**50**); phen = 1,10-phenanthroline), have been reported.²⁵⁵ The intra-complex antiferromagnetic interactions are also relatively large, $J_{\text{Mn}-\text{Ni}}/k_{\text{B}} \approx -24$ K, but ac susceptibility measurements reveal SMM properties with $\Delta_{\text{eff}}/k_{\text{B}} \approx 18$ K and $\tau_0 \approx 10^{-7}$ s for both systems. It is worth mentioning that these SMMs are indeed the elementary units of the archetypal single-chain magnets: $[\text{Mn}_2(\text{saltmen})_2\text{Ni}(\text{pao})_2(\text{py})_2](\text{ClO}_4)_2$, and the analogous systems.⁸⁴ In $[\text{Mn}^{\text{III}}_2(5\text{-MeOsaltmen})_2\text{Cu}^{\text{II}}_2\text{L}_2] \cdot (\text{CF}_3\text{SO}_3)_2 \cdot 2\text{H}_2\text{O}$ (**51**; L = 3-{2-[2-hydroxybenzylidene]amino}-2-methyl-propylimino}-butan-2-one-oximate) incorporating a central $\{\text{Mn}_2(\text{SB})_2\}^{2+}$ core decorated by two Cu^{II} -aldoximate

units (Fig. 11), clear SMM properties are detected.²⁵⁶ Similarly, the reaction of a manganese(II) complex $[\text{Mn}^{\text{II}}(5\text{-MeOsaltmen})] \cdot n\text{H}_2\text{O}$ with N,N' -dicyano-1,4naphthoquinonediimine (DCNNQI) affords Mn^{III} -radical complexes with a $[\text{Mn}^{\text{III}}_2(5\text{-MeOsaltmen})_2 \cdot (\text{DCNNQI}^{\bullet-})_2]$ core (**52**).²⁵⁷ The Mn^{III} -radical interaction is antiferromagnetic ($J_{\text{Mn}-\text{rad}}/k_{\text{B}} < -23$ K) and much stronger than the ferromagnetic $\text{Mn}^{\text{III}}-\text{Mn}^{\text{III}}$ interaction ($J_{\text{Mn}-\text{Mn}}/k_{\text{B}} < +2.0$ K) leading to an $S_{\text{T}} = 3$ ground state. The ac susceptibility measurements reveal the SMM properties of these complexes with frequency-dependent in-phase and out-of-phase components ($\nu_{\text{ac}} \leq 1.5$ kHz, $T \geq 1.8$ K) as well as a sweep rate dependence of the M vs. H hysteresis at 0.4 K.

Beside the $\{\text{Mn}(\text{SB})\}^+$ modules, similar acceptor building blocks to design SMMs are relatively rare and only a few other examples, which have already been described in the previous paragraphs, are shown in Scheme 1(l–o). Recently, mononuclear transition metal complexes with “unconventional” coordination numbers and geometries have been reported to display SMM properties due to a very strong magnetic anisotropy.^{40,46,258} This new category of mononuclear SMMs is currently the topic of a very competitive subject with a rapidly growing number of published systems.^{39–48,259} It sounds reasonable to think that in the close future some of these complexes could be employed as acceptors or, in some cases, donor modules to design new polynuclear SMMs with remarkable characteristics.

Lanthanide and actinide based building-blocks

Obtaining a topological control of coordination architectures with f-block elements is notoriously difficult due to their high coordination numbers and the lack of ligand field stabilization. Indeed the coordination geometries are mainly governed by the sterical hindrances of the (metallo-)ligands and crystal packing effects.²⁶⁰ In addition, even very weak ligand field perturbations may have a significantly strong influence on the SMM properties.^{38,261–263} Despite the obvious downsides from the viewpoint of the chemical design, lanthanide-based complexes have received an immense attention in recent years as they have served as key ingredients in several high barrier 3d–4f or pure 4f SMMs.^{71,72,264–266} Although the observation of SMM properties in most lanthanide complexes is inherently related to the ligand field of the isolated lanthanide ion,^{262,263,267,268} effects of even small ligand field perturbations and exchange interactions have shown to be of crucial importance in the observation of magnetization slow dynamics.^{38,269} For these reasons, the molecular design of lanthanide-based SMMs requires the ligand field of the lanthanide ions to be as preserved as possible. This is clearly not an easy task even if the use of multi-dentate chelating ligands or other particularly rigid ligands, with or without functional groups susceptible to bridge adjacent magnetic centers, might be an approach to explore. Recently, Murugesu and Long reported COT-based Er and Dy SMMs (COT = cycloocta-1,3,5,7-tetraenediide), which exhibit M vs. H hysteresis loops at temperatures of up to 10 K (for $[\text{Er}(\text{COT})_2]^-$ with a field sweep rate of 0.78 mT s^{-1}). Indeed such rigid complexes appear to be promising modules for higher-nuclearity systems.³⁶ Although serendipitous approaches have

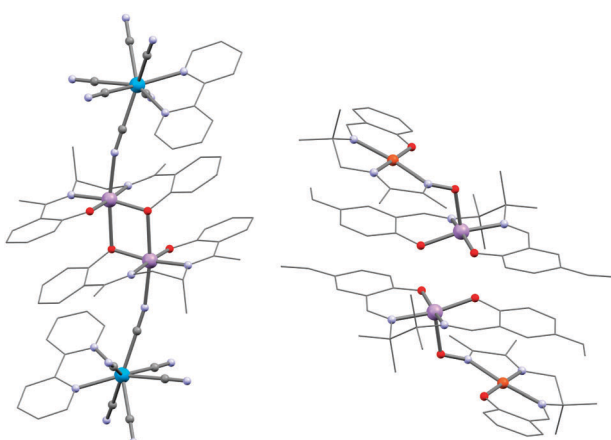


Fig. 11 Structure of **47** (left) and **51** (right). For **51**, the apical $\text{Mn} \cdots \text{O}$ separations are very long (3.081(2) Å) and concomitantly is the $\text{Mn}^{\text{III}}-\text{Mn}^{\text{III}}$ interaction only weak ($J_{\text{Mn}-\text{Mn}}/k_{\text{B}} = +1.7(1)$ K).



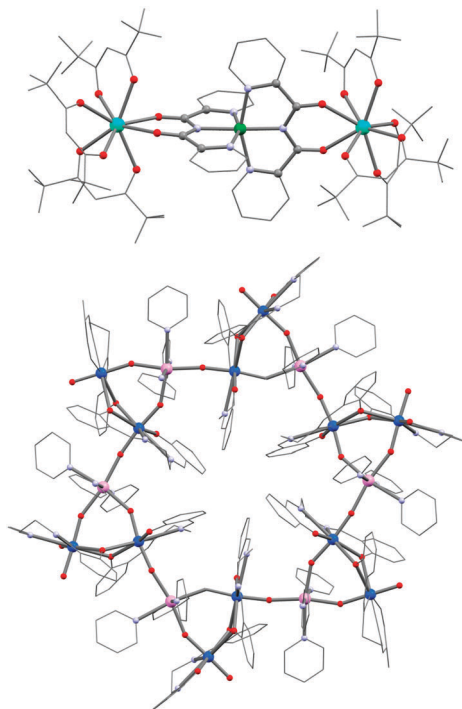


Fig. 12 Molecular structure of **53** (top) and **59** (bottom). U, marine; Dy, pink; Ni, green; Mn, pink; Cr, green; O, red; N, light blue; C, grey.

been used extensively to synthesize 4f metal ion based SMMs,²⁷ lanthanide building blocks do exist and the modular strategy has also been applied successfully to a limited number of systems.^{270,271} A very common building block is the $[\text{Dy}(\text{hfac})_3(\text{H}_2\text{O})_2]$ complex ($\text{hfac} = 1,1,1,5,5,5$ -hexafluoroacetylacetone). The two coordinated water molecules are easily replaced either by azeotropic distillation or directly in the synthesis of polynuclear systems. Lanthanide-based SMM complexes are reported with coordinating nitronyl nitroxide radicals,^{272,273} organic linkers^{274,275} and transition metal complexes.^{276–279} For instance, $[\text{Ni}^{\text{II}}(\text{bpca})_2]$ (Scheme 1g; $\text{Hbpca} = \text{bis}(2\text{-pyridylcarbonyl})\text{amine}$) is able to coordinate bidentately to one or two lanthanide ions in an “acac-like” fashion (Fig. 12).^{280,281} Both $[\text{Dy}(\text{hfac})_3\text{Ni}(\text{bpca})_2\text{Dy}(\text{hfac})_3]\text{CHCl}_3$ (**53**) and the iron(II) analogue **54** incorporating low-spin diamagnetic $[\text{Fe}^{\text{II}}(\text{bpca})_2]$, show SMM properties but the latter has a higher energy barrier (9.7 K vs. 4.9 K) despite the ferromagnetic Dy–Ni interactions in **53**. This result illustrates well that a simple design of lanthanide-based SMMs is currently not easily accessible.

Indeed, only a very few polynuclear lanthanide complexes, which exhibit SMM properties, were obtained using a molecular building block approach. Recent examples are the $\{\text{Dy}_3\text{Co}^{\text{III}}\}$ (**55**) and $\{\text{Dy}_3\text{Fe}^{\text{III}}\}$ (**56**) propellers ($[\text{MDy}_3\text{Tp}_6(\text{dto})_3]\text{4CH}_3\text{CN}\text{2CH}_2\text{Cl}_2$; M = Co^{III} or Fe^{III}; dto = dithiooxalate dianion) reported by Tang and co-workers.²⁸² In these complexes, three dithiooxalate dianions bridge by the sulfur end to the “softer” Co^{III} or Fe^{III} metal ions while the “hard” Dy^{III} sites prefer to coordinate to the donor oxygens (Fig. 10).²⁸² It is worth noting that lanthanide oxalates are extremely insoluble and only one lanthanide-based SMM featuring oxalate bridging has been

reported so far ($[(\text{Tp})_4\text{Dy}_2(\mu\text{-ox})]\text{2CH}_3\text{CN}\text{CH}_2\text{Cl}_2$).²⁸³ Interestingly, the SMM barrier of **55** (52 K) is higher than for the exchange coupled complex **56** that corroborates the argumentation given by Sessoli and co-workers for **53** and **54**.²⁸¹ Winpenny and co-workers have elegantly used Cr^{III} “horseshoe” modules to obtain mixed chromium(III)–lanthanide(III) complexes but none of them were reported to be SMMs.²⁸⁴ Bendix's group has recently demonstrated the possibility of controlling to some extent the topology of lanthanide-based complexes using fluoride bridges.^{232,233,236} The strong preference of fluoride to stabilize linear bridges seems to dictate the polynuclear complex arrangement.^{231,234} For instance, *cis*-difluoride, *trans*-difluoride and *fac*-trifluoride complexes can form linear rod-like, square-like and pyramidal molecular systems, respectively, which show SMM properties for some of them.^{230,232} As an illustration, the trinuclear fluoride-bridged SMM (**57**), $[\text{Dy}(\text{hfac})_3(\text{H}_2\text{O})\text{CrF}_2(\text{py})_4\text{Dy}(\text{hfac})_3(\text{NO}_3)]$, is obtained from the assembly of *trans*- $[\text{CrF}_2(\text{py})_4]^+$ and $[\text{Dy}(\text{hfac})_3(\text{H}_2\text{O})_2]$ modules. The magnetization dynamics was too fast to be able to observe a χ'' maximum (with $\nu_{\text{ac}} \leq 1.5$ kHz), but muon-spin rotation spectroscopy reveals a small energy barrier of about 4.2 K ($\tau_0 = 5.3(4) \times 10^{-8}$ s). In addition, the study of **57** by X-ray magnetic circular dichroism allowed a direct estimation of the nature and magnitude of the exchange interaction.²³³ This information can hardly be obtained from bulk magnetic measurements and is therefore, generally, not known for lanthanide SMMs.²⁸⁰

Actinide based complexes are gaining an increasing attention in the SMM community due to their strong magnetic anisotropy, like lanthanide ions, but also because they offer the possibility of stronger exchange interaction due to the less localized 5f orbitals over the 4f orbitals of the lanthanides.²⁸⁵ Until now, actinide SMMs are known only for U and Np systems. But most of the few published studies have been dedicated to mononuclear U^{III} systems^{286–290} for which it was recently argued that the SMM properties are intrinsic to the trivalent uranium centre.²⁹¹ A single example of a mononuclear Np^{IV} system has been reported: neptunocene, $[\text{Np}(\text{COT})_2]$ (**58**).²⁹² Only two examples of exchange coupled polynuclear uranium SMMs are reported so far.^{293,294} The first one reported by Liddle and co-workers is an inverted-sandwich arene-bridged diuranium(III) species that shows a frequency dependent ac susceptibility signal below 5 K.²⁹³ The second example is an U^V-based $\{\text{Mn}^{\text{II}}_6\text{U}^{\text{V}}_{12}\}$ wheel complex (**59**; $[(\text{UO}_2(\text{salen})]_{12-}\text{Mn}(\text{py})_3)_6$; Fig. 12) prepared by one-electron reduction of $[\text{U}^{\text{VI}}\text{O}_2(\text{salen})]$ with $[\text{Co}^{\text{II}}\text{Cp}^*]$ ($\text{Cp}^* = \text{pentamethylcyclopentadienide}$) and subsequent assembly with Mn^{II} metal ions.²⁹⁴ The six-coordinate $[\text{U}^{\text{VI}}\text{O}_2(\text{salen})]^-$ unit dimerizes to form an approximate pentagonal bipyramidal local symmetry around the U^V sites. This complex exhibits an *M* vs. *H* hysteresis loop below 4 K (with an 4 mT s⁻¹ average field sweep rate) and a relaxation time that is thermally activated with a large barrier of 142(7) K and a very small $\tau_0 = 3(2) \times 10^{-12}$ s. In 2010, Magnani and co-workers reported the first neptunium SMM, $\{\text{Np}^{\text{VI}}\text{O}_2\text{Cl}_2\}\{\text{Np}^{\text{V}}\text{O}_2\text{Cl}(\text{THF})_3\}_2$ (**60**), exhibiting an exotic trinuclear neptunium(V,VI) core. The slow dynamics of the

magnetization of this complex was studied using the ac technique leading to an 140-K energy barrier.^{50,295}

5. Conclusions and perspectives

Combining relevant and interesting physical properties in a controlled manner in the same material is an important topic for modern chemists. In particular, the engineering of new multifunctional materials associating magnetism with *e.g.* photo-activity, electro-activity, porosity, conductivity or other properties controlled by an external stimuli, are being currently targeted by many research groups. Potentially, coordination chemistry provides the necessary tools for designing such new materials in rational and methodical approaches. However, the development of the preparative coordination chemistry is still behind the organic chemistry and consequently, it remains difficult for coordination chemists to design and synthesize, at will, polynuclear metal ion complexes or coordination polymers. Inspired from the protective groups in organic chemistry that direct the reactivity in particular positions, coordination chemists increase their structural control on the final material by using precursors with reduced degrees of freedom. Along this line, the used building-blocks are often carrying capping or strongly coordinating ligands to be able to direct the coordination properties and the final assemblies. Nevertheless, it is important to keep in mind that serendipitous self-assembly reactions have provided many systems of crucial importance to the development of the field of molecular magnetism and that the limitations of the modular approach with respect to structural design of polynuclear complexes are still important.

By creating complicated structures in a hierarchical fashion, the preparative coordination chemist can rely on an existing understanding of the first and second coordination sphere complexations and the well-understood relative robustness of coordination complexes. Furthermore, this modular strategy offers an efficient transfer of the metal ion properties, imposed by the first coordination sphere, to extended structures. Thus, this approach allows us to control not only the spatial arrangements, but also the electronic structure of complicated systems. In this context, many combinations of metal ion modules and bridging ligands are unexplored to design new molecule-based magnetic materials including SMMs and related materials.

In parallel with the use of known building-blocks, the quest for new magnetic modules should not be forgotten as they constitute the basis of this synthetic strategy. In particular, it would be very interesting to exploit the recent examples of mononuclear SMMs and photo-switchable SMMs as modules for higher nuclearity SMM-based architectures. As evidenced in this Feature article by the current limited number of modules used to elaborate SMMs, chemists should continue to develop this step-by-step approach in concert with more serendipitous syntheses, which have led, and will also lead, to many magnetically interesting systems without clearly identified building-block precursors. However, we believe that the described modular

synthetic strategy, that efficiently used the existing knowledge of coordination chemistry, offers the best chances to premeditate and control the physical properties of the resulting coordination structures.

Acknowledgements

We are grateful to all our co-workers, past students and friends who have contributed to our scientific adventures. Special thanks to Dr D. Woodruff for valuable discussions. In addition, the authors thank the Danish Ministry of Science, Innovation and Higher Education for the EliteForsk travel stipend to K.S.P., the Conseil Régional d'Aquitaine, the Université of Bordeaux, the Danish research Councils, the French Embassy in Denmark (IFD, French-Danish Research Collaboration Program), the CNRS and the ANR.

Notes and references

- 1 R. Sessoli, D. Gatteschi, A. Caneschi and M. A. Novak, *Nature*, 1993, **365**, 141–143.
- 2 D. Gatteschi and R. Sessoli, *Angew. Chem., Int. Ed.*, 2003, **42**, 268–297.
- 3 G. Aromi and E. K. Brechin, in *Single-Molecule Magnets and Related Phenomena*, ed. R. Winpenny, 2006, pp. 1–67.
- 4 G. Christou, D. Gatteschi, D. N. Hendrickson and R. Sessoli, *MRS Bull.*, 2000, **25**, 66–71.
- 5 R. Sessoli, H. L. Tsai, A. R. Schake, S. Y. Wang, J. B. Vincent, K. Folting, D. Gatteschi, G. Christou and D. N. Hendrickson, *J. Am. Chem. Soc.*, 1993, **115**, 1804–1816.
- 6 M. N. Leuenberger and D. Loss, *Nature*, 2001, **410**, 789–793.
- 7 L. Bogani and W. Wernsdorfer, *Nat. Mater.*, 2008, **7**, 179–186.
- 8 J. Lehmann, A. Gaita-Ariño, E. Coronado and D. Loss, *J. Mater. Chem.*, 2009, **19**, 1672–1677.
- 9 J. Camarero and E. Coronado, *J. Mater. Chem.*, 2009, **19**, 1678–1684.
- 10 D. Gatteschi, A. Cornia, M. Mannini and R. Sessoli, *Inorg. Chem.*, 2009, **48**, 3408–3419.
- 11 A. Cornia, M. Mannini, P. Sainctavit and R. Sessoli, *Chem. Soc. Rev.*, 2011, **40**, 3076–3091.
- 12 M. Mannini, F. Pineider, P. Sainctavit, C. Danieli, E. Otero, C. Sciancalepore, A. M. Talarico, M. A. Arrio, A. Cornia, D. Gatteschi and R. Sessoli, *Nat. Mater.*, 2009, **8**, 194–197.
- 13 M. Mannini, F. Pineider, C. Danieli, F. Totti, L. Sorace, P. Sainctavit, M. A. Arrio, E. Otero, L. Joly, J. C. Cezar, A. Cornia and R. Sessoli, *Nature*, 2010, **468**, 417–421.
- 14 C. Schlegel, E. Burzurí, F. Luis, F. Moro, M. Manoli, E. K. Brechin, M. Murrie and J. van Slageren, *Chem.-Eur. J.*, 2010, **16**, 10178–10185.
- 15 R. Inglis, J. Béndix, T. Brock-Nannestad, H. Weihe, E. K. Brechin and S. Piligkos, *Chem. Sci.*, 2010, **1**, 631–636.
- 16 A. Cornia, A. F. Costantino, L. Zobbi, A. Caneschi, D. Gatteschi, M. Mannini and R. Sessoli, in *Single-Molecule Magnets and Related Phenomena*, ed. R. Winpenny, Springer-Verlag Berlin, Berlin, 2006, pp. 133–161.
- 17 N. Domingo, E. Bellido and D. Ruiz-Molina, *Chem. Soc. Rev.*, 2012, **41**, 258–302.
- 18 R. Vincent, S. Klyatskaya, M. Ruben, W. Wernsdorfer and F. Balestro, *Nature*, 2012, **488**, 357–360.
- 19 M. Clemente-León, H. Soyer, E. Coronado, C. Mingotaud, C. J. Gómez-García and P. Delhaès, *Angew. Chem., Int. Ed.*, 1998, **37**, 2842–2845.
- 20 T. Coradin, J. Larionova, A. A. Smith, G. Rogez, R. Clérac, C. Guérin, G. Blondin, R. E. P. Winpenny, C. Sanchez and T. Mallah, *Adv. Mater.*, 2002, **14**, 896–898.
- 21 C. Coulon, H. Miyasaka and R. Clérac, in *Single-Molecule Magnets and Related Phenomena*, ed. R. Winpenny, 2006, pp. 163–206.
- 22 I.-R. Jeon and R. Clérac, *Dalton Trans.*, 2012, **41**, 9569–9586.



23 L. Bogani, A. Vindigni, R. Sessoli and D. Gatteschi, *J. Mater. Chem.*, 2008, **18**, 4750–4758.

24 H.-L. Sun, Z.-M. Wang and S. Gao, *Coord. Chem. Rev.*, 2010, **254**, 1081–1100.

25 W.-X. Zhang, R. Ishikawa, B. K. Breedlove and M. Yamashita, *RSC Adv.*, 2012, **3**, 3772–3798.

26 N. Ishikawa, M. Sugita, T. Ishikawa, S. Koshihara and Y. Kaizu, *J. Am. Chem. Soc.*, 2003, **125**, 8694–8695.

27 D. N. Woodruff, R. E. P. Winpenny and R. A. Layfield, *Chem. Rev.*, 2013, **113**, 5110–5148.

28 M. A. AlDamen, J. M. Clemente-Juan, E. Coronado, C. Martí-Gastaldo and A. Gaita-Ariño, *J. Am. Chem. Soc.*, 2008, **130**, 8874–8875.

29 P.-E. Car, M. Perfetti, M. Mannini, A. Favre, A. Caneschi and R. Sessoli, *Chem. Commun.*, 2011, **47**, 3751–3753.

30 S.-D. Jiang, B.-W. Wang, H.-L. Sun, Z.-M. Wang and S. Gao, *J. Am. Chem. Soc.*, 2011, **133**, 4730–4733.

31 S.-D. Jiang, B.-W. Wang, G. Su, Z.-M. Wang and S. Gao, *Angew. Chem., Int. Ed.*, 2010, **49**, 7448–7451.

32 M.-E. Boulon, G. Cucinotta, J. Luzon, C. Degl'Innocenti, M. Perfetti, K. Bernot, G. Calvez, A. Caneschi and R. Sessoli, *Angew. Chem., Int. Ed.*, 2013, **52**, 350–354.

33 J.-L. Liu, K. Yuan, J.-D. Leng, L. Ungur, W. Wernsdorfer, F.-S. Guo, L. F. Chibotaru and M.-L. Tong, *Inorg. Chem.*, 2012, **51**, 8538–8544.

34 K. R. Meihaus, J. D. Rinehart and J. R. Long, *Inorg. Chem.*, 2011, **50**, 8484–8489.

35 M. A. AlDamen, S. Cardona-Serra, J. M. Clemente-Juan, E. Coronado, A. Gaita-Ariño, C. Martí-Gastaldo, F. Luis and O. Montero, *Inorg. Chem.*, 2009, **48**, 3467–3479.

36 J. J. Le Roy, M. Jeletic, S. I. Gorelsky, I. Korobkov, L. Ungur, L. F. Chibotaru and M. Murugesu, *J. Am. Chem. Soc.*, 2013, **135**, 3502–3510; K. R. Meihaus and J. R. Long, *J. Am. Chem. Soc.*, 2013, **135**, 17952–17957; J. J. Le Roy, I. Korobkov and M. Murugesu, *Chem. Commun.*, 2014, **50**, 1602–1604.

37 E. Lucaccini, L. Sorace, M. Perfetti, J.-P. Costes and R. Sessoli, *Chem. Commun.*, 2014, **50**, 1648–1651.

38 K. S. Pedersen, L. Ungur, M. Sigrist, A. Sundt, M. Schau-Magnussen, V. Vieru, H. Mutka, S. Rols, H. Weihe, O. Waldmann, L. Chibotaru, J. Bendix and J. Dreiser, *Chem. Sci.*, 2014, **5**, 1650–1660.

39 W. H. Harman, T. D. Harris, D. E. Freedman, H. Fong, A. Chang, J. D. Rinehart, A. Ozarowski, M. T. Sougrati, F. Grandjean, G. J. Long, J. R. Long and C. J. Chang, *J. Am. Chem. Soc.*, 2010, **132**, 18115–18126.

40 J. M. Zadrozny, M. Atanasov, A. M. Bryan, C.-Y. Lin, B. D. Rekken, P. P. Power, F. Neese and J. R. Long, *Chem. Sci.*, 2013, **4**, 125–138.

41 D. E. Freedman, W. H. Harman, T. D. Harris, G. J. Long, C. J. Chang and J. R. Long, *J. Am. Chem. Soc.*, 2010, **132**, 1224–1225.

42 P.-H. Lin, N. C. Smythe, S. I. Gorelsky, S. Maguire, N. J. Henson, I. Korobkov, B. L. Scott, J. C. Gordon, R. T. Baker and M. Murugesu, *J. Am. Chem. Soc.*, 2011, **133**, 15806–15809.

43 J. M. Zadrozny and J. R. Long, *J. Am. Chem. Soc.*, 2011, **133**, 20732–20734.

44 S. Mossin, B. L. Tran, D. Adhikari, M. Pink, F. W. Heinemann, J. Sutter, R. K. Szilagyi, K. Meyer and D. J. Mindiola, *J. Am. Chem. Soc.*, 2012, **134**, 13651–13661.

45 Y.-Y. Zhu, C. Cui, Y.-Q. Zhang, J.-H. Jia, X. Guo, C. Gao, K. Qian, S.-D. Jiang, B.-W. Wang, Z.-M. Wang and S. Gao, *Chem. Sci.*, 2013, **4**, 1802–1806.

46 J. M. Zadrozny, D. J. Xiao, M. Atanasov, G. J. Long, F. Grandjean, F. Neese and J. R. Long, *Nat. Chem.*, 2013, **5**, 577–581.

47 F. Habib, O. R. Luca, V. Vieru, M. Shiddiq, I. Korobkov, S. I. Gorelsky, M. K. Takase, L. F. Chibotaru, S. Hill, R. H. Crabtree and M. Murugesu, *Angew. Chem., Int. Ed.*, 2013, **52**, 11290–11293.

48 J. M. Zadrozny, J. Telser and J. R. Long, *Polyhedron*, 2013, **64**, 209–217.

49 X. Feng, C. Mathonière, I.-R. Jeon, M. Rouzières, A. Ozarowski, M. L. Aubrey, M. I. Gonzalez, R. Clérac and J. R. Long, *J. Am. Chem. Soc.*, 2013, **135**, 15880–15884.

50 C. Mathonière, H.-J. Lin, D. Siretanu, R. Clérac and J. M. Smith, *J. Am. Chem. Soc.*, 2013, **135**, 19083–19086.

51 T. Lis, *Acta Crystallogr., Sect. B: Struct. Crystallogr. Cryst. Chem.*, 1980, **36**, 2042–2046.

52 R. Bagai and G. Christou, *Chem. Soc. Rev.*, 2009, **38**, 1011–1026.

53 R. E. P. Winpenny, *J. Chem. Soc., Dalton Trans.*, 2002, 1–10.

54 L. Thomas, F. Lionti, R. Ballou, D. Gatteschi, R. Sessoli and B. Barbara, *Nature*, 1996, **383**, 145–147.

55 W. Wernsdorfer and R. Sessoli, *Science*, 1999, **284**, 133–135.

56 D. Gatteschi, R. Sessoli and J. Villain, *Molecular Nanomagnets*, Oxford University Press, New York, 2006.

57 J. M. Zadrozny, J. Liu, N. A. Piro, C. J. Chang, S. Hill and J. R. Long, *Chem. Commun.*, 2012, **48**, 3927–3929.

58 J. Vallejo, I. Castro, R. Ruiz-García, J. Cano, M. Julve, F. Lloret, G. De Munno, W. Wernsdorfer and E. Pardo, *J. Am. Chem. Soc.*, 2012, **134**, 15704–15707.

59 E. Colacio, J. Ruiz, E. Ruiz, E. Cremades, J. Krzystek, S. Carretta, J. Cano, T. Guidi, W. Wernsdorfer and E. K. Brechin, *Angew. Chem., Int. Ed.*, 2013, **52**, 9130–9134.

60 K. S. Pedersen, M. Sigrist, M. A. Sørensen, A. L. Barra, T. Weyhermueller, S. Piligkos, C. A. Thuesen, M. G. Vinum, H. Mutka, H. Weihe, R. Clérac and J. Bendix, *Angew. Chem., Int. Ed.*, 2014, **53**, 1351–1354.

61 H. Miyasaka, R. Clérac, W. Wernsdorfer, L. Lecren, C. Bonhomme, K. Sugiura and M. Yamashita, *Angew. Chem., Int. Ed.*, 2004, **43**, 2801–2805.

62 J. Villain, F. Hartman-Boutron, R. Sessoli and A. Rettori, *Europhys. Lett.*, 1994, **27**, 159–164.

63 A. J. Tasiopoulos, A. Vinslava, W. Wernsdorfer, K. A. Abboud and G. Christou, *Angew. Chem., Int. Ed.*, 2004, **43**, 2117–2121.

64 A. M. Ako, I. J. Hewitt, V. Mereacre, R. Clérac, W. Wernsdorfer, C. E. Anson and A. K. Powell, *Angew. Chem., Int. Ed.*, 2006, **45**, 4926–4929.

65 O. Waldmann, A. M. Ako, H. U. Güdel and A. K. Powell, *Inorg. Chem.*, 2008, **47**, 3486–3488.

66 C. J. Milios, A. Vinslava, W. Wernsdorfer, S. Moggach, S. Parsons, S. P. Perlepes, G. Christou and E. K. Brechin, *J. Am. Chem. Soc.*, 2007, **129**, 2754–2755.

67 C. J. Milios, R. Inglis, A. Vinslava, R. Bagai, W. Wernsdorfer, S. Parsons, S. P. Perlepes, G. Christou and E. K. Brechin, *J. Am. Chem. Soc.*, 2007, **129**, 12505–12511.

68 O. Waldmann, *Inorg. Chem.*, 2007, **46**, 10035–10037.

69 F. Neese and D. A. Pantazis, *Faraday Discuss.*, 2011, **148**, 229–238.

70 E. Ruiz, J. Cirera, J. Cano, S. Alvarez, C. Loose and J. Kortus, *Chem. Commun.*, 2008, 52–54.

71 J. D. Rinehart, M. Fang, W. J. Evans and J. R. Long, *J. Am. Chem. Soc.*, 2011, **133**, 14236–14239.

72 J. D. Rinehart, M. Fang, W. J. Evans and J. R. Long, *Nat. Chem.*, 2011, **3**, 538–542.

73 R. J. Blagg, L. Ungur, F. Tuna, J. Speak, P. Comar, D. Collison, W. Wernsdorfer, E. J. L. McInnes, L. F. Chibotaru and R. E. P. Winpenny, *Nat. Chem.*, 2013, **5**, 673–678.

74 L. M. C. Beltran and J. R. Long, *Acc. Chem. Res.*, 2005, **38**, 325–334.

75 F. Allen, *Acta Crystallogr., Sect. A: Fundam. Crystallogr.*, 2002, **58**, 380–388.

76 M. Shatruk, C. Avendano and K. R. Dunbar, in *Prog. Inorg. Chem.*, ed. K. D. Karlin, 2009, vol. 56, pp. 155–334.

77 J. L. Heinrich, P. A. Berseth and J. R. Long, *Chem. Commun.*, 1998, 1231–1232.

78 M. Affronte, S. Carretta, G. A. Timco and R. E. P. Winpenny, *Chem. Commun.*, 2007, 1789–1797.

79 R. E. P. Winpenny, *Adv. Inorg. Chem.*, 2001, **52**, 1–111.

80 G. Aromi, S. M. J. Aubin, M. A. Bolcar, G. Christou, H. J. Eppley, K. Folting, D. N. Hendrickson, J. C. Huffman, R. C. Squire, H. L. Tsai, S. Wang and M. W. Wemple, *Polyhedron*, 1998, **17**, 3005–3020.

81 P. Zhang, Y.-N. Guo and J. Tang, *Coord. Chem. Rev.*, 2013, **257**, 1728–1763.

82 G. E. Kostakis, A. M. Ako and A. K. Powell, *Chem. Soc. Rev.*, 2010, **39**, 2238–2271.

83 A. Caneschi, D. Gatteschi, N. Lalioti, C. Sangregorio, R. Sessoli, G. Venturi, A. Vindigni, A. Rettori, M. G. Pini and M. A. Novak, *Angew. Chem., Int. Ed.*, 2001, **40**, 1760–1763.

84 R. Clérac, H. Miyasaka, M. Yamashita and C. Coulon, *J. Am. Chem. Soc.*, 2002, **124**, 12837–12844.

85 H. Miyasaka, M. Julve, M. Yamashita and R. Clérac, *Inorg. Chem.*, 2009, **48**, 3420–3437.

86 H. Miyasaka and R. Clérac, *Bull. Chem. Soc. Jpn.*, 2005, **78**, 1725–1748.





87 H. Miyasaka, R. Clérac, K. Mizushima, K. Sugiura, M. Yamashita, W. Wernsdorfer and C. Coulon, *Inorg. Chem.*, 2003, **42**, 8203–8213.

88 M. Ferbinteanu, H. Miyasaka, W. Wernsdorfer, K. Nakata, K. Sugiura, M. Yamashita, C. Coulon and R. Clérac, *J. Am. Chem. Soc.*, 2005, **127**, 3090–3099.

89 H. Miyasaka, A. Saitoh, M. Yamashita and R. Clérac, *Dalton Trans.*, 2008, 2422–2427.

90 W. R. Entley and G. S. Girolami, *Science*, 1995, **268**, 397–400.

91 M. Verdaguer, A. Bleuzen, V. Marvaud, J. Vaissermann, M. Seuleiman, C. Desplanches, A. Scuiller, C. Train, R. Garde, G. Gelly, C. Lomenech, I. Rosenman, P. Veillet, C. Cartier and F. Villain, *Coord. Chem. Rev.*, 1999, **192**, 1023–1047.

92 J. S. Miller and J. L. Manson, *Acc. Chem. Res.*, 2001, **34**, 563–570.

93 H. Weihe and H. U. Güdel, *Comments Inorg. Chem.*, 2000, **22**, 75–103.

94 D. Visinescu, C. Desplanches, I. Imaz, V. Bahers, R. Pradhan, F. A. Villamena, P. Guionneau and J. P. Sutter, *J. Am. Chem. Soc.*, 2006, **128**, 10202–10212.

95 D. E. Freedman, D. M. Jenkins and J. R. Long, *Chem. Commun.*, 2009, 4829–4831.

96 T. D. Harris, C. Coulon, R. Clérac and J. R. Long, *J. Am. Chem. Soc.*, 2011, **133**, 123–130.

97 O. Sato, T. Iyoda, A. Fujishima and K. Hashimoto, *Science*, 1996, **272**, 704–705.

98 F. Tuyeras, A. Scuiller, C. Duhayon, M. Hernandez-Molina, F. F. de Biani, M. Verdaguer, T. Mallah, W. Wernsdorfer and V. Marvaud, *Inorg. Chim. Acta*, 2008, **361**, 3505–3518.

99 V. Marvaud, C. Decroix, A. Scuiller, C. Guyard-Duhayon, J. Vaissermann, F. Gonnet and M. Verdaguer, *Chem.-Eur. J.*, 2003, **9**, 1677–1691.

100 J. N. Reilly and T. Mallah, in *Single-Molecule Magnets and Related Phenomena*, ed. R. Winpenny, 2006, pp. 103–131.

101 A. G. Sharpe, *The Chemistry of Cyano Complexes of the Transition Metals*, Academic Press, New York, 1976.

102 W. R. Entley, C. R. Treadway, S. R. Wilson and G. S. Girolami, *J. Am. Chem. Soc.*, 1997, **119**, 6251–6258.

103 K. J. Nelson, I. D. Giles, S. A. Troff, A. M. Arif and J. S. Miller, *Inorg. Chem.*, 2006, **45**, 8922–8929.

104 L. G. Beauvais and J. R. Long, *J. Am. Chem. Soc.*, 2002, **124**, 2110–2111.

105 J. Bendix, P. Steenberg and I. Søtofte, *Inorg. Chem.*, 2003, **42**, 4510–4512.

106 P. Albores, L. D. Slep, L. M. Baraldo, R. Baggio, M. T. Garland and E. Rentschler, *Inorg. Chem.*, 2006, **45**, 2361–2363.

107 T. L. Pappenhagen and D. W. Margerum, *J. Am. Chem. Soc.*, 1985, **107**, 4576–4577.

108 J. B. Goodenough, *Magnetism and the Chemical Bond*, Interscience, New York, 1963.

109 T. Mallah, C. Auberger, M. Verdaguer and P. Veillet, *J. Chem. Soc., Chem. Commun.*, 1995, 61–62.

110 C. P. Berlinguette, D. Vaughn, C. Canada-Vilalta, J. R. Galan-Mascaro and K. R. Dunbar, *Angew. Chem., Int. Ed.*, 2003, **42**, 1523–1526.

111 K. E. Funck, M. G. Hilfiger, C. P. Berlinguette, M. Shatruk, W. Wernsdorfer and K. R. Dunbar, *Inorg. Chem.*, 2009, **48**, 3438–3452.

112 A. V. Palii, S. M. Ostrovsky, S. I. Klokishner, B. S. Tsukerblat, C. P. Berlinguette, K. R. Dunbar and J. R. Galan-Mascaro, *J. Am. Chem. Soc.*, 2004, **126**, 16860–16867.

113 A. Palii, S. M. Ostrovsky, S. I. Klokishner, B. S. Tsukerblat and K. R. Dunbar, *ChemPhysChem*, 2006, **7**, 871–879.

114 A. Palii, B. Tsukerblat, S. Klokishner, K. R. Dunbar, J. M. Clemente-Juan and E. Coronado, *Chem. Soc. Rev.*, 2011, **40**, 3130–3156.

115 M. G. Hilfiger, M. Chen, T. V. Brinzari, T. M. Nocera, M. Shatruk, D. T. Petasis, J. L. Musfeldt, C. Achim and K. R. Dunbar, *Angew. Chem., Int. Ed.*, 2010, **49**, 1410–1413.

116 P. L. W. Tregenna-Piggott, D. Sheptyakov, L. Keller, S. I. Klokishner, S. M. Ostrovsky, A. V. Palii, O. S. Reu, J. Bendix, T. Brock-Nannestad, K. Pedersen, H. Weihe and H. Mutka, *Inorg. Chem.*, 2009, **48**, 128–137.

117 H. Miyasaka, H. Ieda, N. Matsumoto, N. Re, R. Crescenzi and C. Floriani, *Inorg. Chem.*, 1998, **37**, 255–263.

118 H. J. Choi, J. J. Sokol and J. R. Long, *Inorg. Chem.*, 2004, **43**, 1606–1608.

119 H. J. Choi, J. J. Sokol and J. R. Long, *J. Phys. Chem. Solids*, 2004, **65**, 839–844.

120 H. Miyasaka, A. Saitoh and S. Abe, *Coord. Chem. Rev.*, 2007, **251**, 2622–2664.

121 J. Dreiser, A. Schnegg, K. Holldack, K. S. Pedersen, M. Schau-Magnussen, J. Nehrkorn, P. Tregenna-Piggott, H. Mutka, H. Weihe, J. Bendix and O. Waldmann, *Chem.-Eur. J.*, 2011, **17**, 7492–7498.

122 K. S. Pedersen, M. Schau-Magnussen, J. Bendix, H. Weihe, A. V. Palii, S. I. Klokishner, S. Ostrovsky, O. S. Reu, H. Mutka and P. L. W. Tregenna-Piggott, *Chem.-Eur. J.*, 2010, **16**, 13458–13464.

123 K. S. Pedersen, J. Dreiser, J. Nehrkorn, M. Gysler, M. Schau-Magnussen, A. Schnegg, K. Holldack, R. Bittl, S. Piligkos, H. Weihe, P. Tregenna-Piggott, O. Waldmann and J. Bendix, *Chem. Commun.*, 2011, **47**, 6918–6920.

124 K. S. Pedersen, M. Sigrist, H. Weihe, P. L. W. Tregenna-Piggott, M. Schau-Magnussen, J. Dreiser, H. Mutka, A.-L. Barra and J. Bendix, *Inorg. Chem. Commun.*, 2012, **24**, 24–28.

125 A. Palii, B. Tsukerblat, J. M. Clemente-Juan and E. Coronado, *Int. Rev. Phys. Chem.*, 2010, **29**, 135–230.

126 V. S. Mironov, *Dokl. Phys. Chem.*, 2006, **408**, 130–136.

127 A. V. Palii, O. S. Reu, S. M. Ostrovsky, S. I. Klokishner, B. S. Tsukerblat, M. Hilfiger, M. Shatruk, A. Prosvirin and K. R. Dunbar, *J. Phys. Chem. A*, 2009, **113**, 6886–6890.

128 J. S. Griffith, *The Theory of Transition Metal Ions*, Cambridge University Press, Cambridge, 1961.

129 J. Dreiser, K. S. Pedersen, A. Schnegg, K. Holldack, J. Nehrkorn, M. Sigrist, P. Tregenna-Piggott, H. Mutka, H. Weihe, V. S. Mironov, J. Bendix and O. Waldmann, *Chem.-Eur. J.*, 2013, **19**, 3693–3701.

130 J. Larionova, B. Mombelli, J. Sanchiz and O. Kahn, *Inorg. Chem.*, 1998, **37**, 679–684.

131 J. Bendix, M. Brorson and C. E. Schäffer, *Inorg. Chem.*, 1993, **32**, 2838–2849.

132 M. Atanasov, C. Busche, P. Comba, F. El Hallak, B. Martin, G. Rajaraman, J. van Slageren and H. Wadeppohl, *Inorg. Chem.*, 2008, **47**, 8112–8125.

133 X.-Y. Wang, C. Avendano and K. R. Dunbar, *Chem. Soc. Rev.*, 2011, **40**, 3213–3238.

134 H. Miyasaka, H. Takahashi, T. Madanbashi, K. Sugiura, R. Clérac and H. Nojiri, *Inorg. Chem.*, 2005, **44**, 5969–5971.

135 Y.-Z. Zhang, B.-W. Wang, O. Sato and S. Gao, *Chem. Commun.*, 2010, **46**, 6959–6961.

136 T. Glaser, M. Heidemeier, T. Weyhermüller, R.-D. Hoffmann, H. Rupp and P. Müller, *Angew. Chem., Int. Ed.*, 2006, **45**, 6033–6037.

137 T. Glaser, *Chem. Commun.*, 2011, **47**, 116–130.

138 V. Hoeke, E. Krickemeyer, M. Heidemeier, H. Theil, A. Stammmer, H. Bögge, T. Weyhermüller, J. Schnack and T. Glaser, *Eur. J. Inorg. Chem.*, 2013, 4398–4409.

139 V. Hoeke, A. Stammmer, H. Bögge, J. Schnack and T. Glaser, *Inorg. Chem.*, 2013, **53**, 257–268.

140 V. Hoeke, K. Gieb, P. Müller, L. Ungur, L. Chibotaru, M. Heidemeier, E. Krickemeyer, A. Stammmer, H. Bögge, C. Schröder, J. Schnack and T. Glaser, *Chem. Sci.*, 2012, **3**, 2868–2882.

141 V. Hoeke, M. Heidemeier, E. Krickemeyer, A. Stammmer, H. Bögge, J. Schnack and T. Glaser, *Dalton Trans.*, 2012, **41**, 12942–12959.

142 D. E. Freedman, D. M. Jenkins, A. T. Iavarone and J. R. Long, *J. Am. Chem. Soc.*, 2008, **130**, 2884–2885.

143 J. M. Zadrożny, D. E. Freedman, D. M. Jenkins, T. D. Harris, A. T. Iavarone, C. Mathonière, R. Clérac and J. R. Long, *Inorg. Chem.*, 2010, **49**, 8886–8896.

144 M. V. Bennett and J. R. Long, *J. Am. Chem. Soc.*, 2003, **125**, 2394–2395.

145 V. S. Mironov, L. F. Chibotaru and A. Ceulemans, *J. Am. Chem. Soc.*, 2003, **125**, 9750–9760.

146 X.-Y. Wang, A. V. Prosvirin and K. R. Dunbar, *Angew. Chem., Int. Ed.*, 2010, **49**, 5081–5084.

147 K. Qian, X.-C. Huang, C. Zhou, X.-Z. You, X.-Y. Wang and K. R. Dunbar, *J. Am. Chem. Soc.*, 2013, **135**, 13302–13305.

148 P. Przychodzeń, T. Korzeniak, R. Podgajny and B. Sieklucka, *Coord. Chem. Rev.*, 2006, **250**, 2234–2260.

149 B. Nowicka, T. Korzeniak, O. Stefańczyk, D. Pinkowicz, S. Chorzy, R. Podgajny and B. Sieklucka, *Coord. Chem. Rev.*, 2012, **256**, 1946–1971.

150 B. Sieklucka, R. Podgajny, P. Przychodzeń and T. Korzeniak, *Coord. Chem. Rev.*, 2005, **249**, 2203–2221.

151 B. Sieklucka, R. Podgajny, D. Pinkowicz, B. Nowicka, T. Korzeniak, M. Balandz, T. Wasilutynski, R. Pelka, M. Makarewicz, M. Czapla, M. Rams, B. Gawel and W. Lasocha, *CrystEngComm*, 2009, **11**, 2032–2039.

152 M. G. Hilfiger, H. Zhao, A. Prosvirin, W. Wernsdorfer and K. R. Dunbar, *Dalton Trans.*, 2009, 5155–5163.

153 J. H. Lim, H. S. Yoo, J. H. Yoon, E. K. Koh, H. C. Kim and C. S. Hong, *Polyhedron*, 2008, **27**, 299–303.

154 J. H. Lim, J. H. Yoon, H. C. Kim and C. S. Hong, *Angew. Chem., Int. Ed.*, 2006, **45**, 7424–7426.

155 D. E. Freedman, M. V. Bennett and J. R. Long, *Dalton Trans.*, 2006, 2829–2834.

156 J.-P. Sutter, S. Dhers, J.-P. Costes and C. Duhayon, *C. R. Chim.*, 2008, **11**, 1200–1206.

157 J. Long, L.-M. Chamoreau and V. Marvaud, *Dalton Trans.*, 2010, **39**, 2188–2190.

158 M. Koziel, R. Pelka, M. Rams, W. Nitek and B. Sieklucka, *Inorg. Chem.*, 2010, **49**, 4268–4277.

159 S. Dhers, S. Sahoo, J.-P. Costes, C. Duhayon, S. Ramasesha and J.-P. Sutter, *CrystEngComm*, 2009, **11**, 2078–2083.

160 J.-P. Sutter, S. Dhers, R. Rajamani, S. Ramasesha, J.-P. Costes, C. Duhayon and L. Vendier, *Inorg. Chem.*, 2009, **48**, 5820–5828.

161 D. Visinescu, I.-R. Jeon, A. M. Madalan, M.-G. Alexandru, B. Jurca, C. Mathonière, R. Clérac and M. Andruh, *Dalton Trans.*, 2012, **41**, 13578–13581.

162 J.-P. Costes, F. Dahan, A. Dupuis and J.-P. Laurent, *Inorg. Chem.*, 1996, **35**, 2400–2402.

163 M. Andruh, *Chem. Commun.*, 2011, **47**, 3025–3042.

164 S. Wang, X. H. Ding, Y. H. Li and W. Huang, *Coord. Chem. Rev.*, 2012, **256**, 439–464.

165 S. Wang, X. H. Ding, J. L. Zuo, X. Z. You and W. Huang, *Coord. Chem. Rev.*, 2011, **255**, 1713–1732.

166 J. J. Sokol, A. G. Hee and J. R. Long, *J. Am. Chem. Soc.*, 2002, **124**, 7656–7657.

167 J. L. Heinrich, J. J. Sokol, A. G. Hee and J. R. Long, *J. Solid State Chem.*, 2001, **159**, 293–301.

168 B. N. Figgis, *Trans. Faraday Soc.*, 1960, **56**, 1553–1558.

169 T. D. Harris, M. V. Bennett, R. Clérac and J. R. Long, *J. Am. Chem. Soc.*, 2010, **132**, 3980–3988.

170 X. W. Feng, J. J. Liu, T. D. Harris, S. Hill and J. R. Long, *J. Am. Chem. Soc.*, 2012, **134**, 7521–7529.

171 X. Feng, T. David Harris and J. R. Long, *Chem. Sci.*, 2011, **2**, 1688–1694.

172 T. D. Harris, H. S. Soo, C. J. Chang and J. R. Long, *Inorg. Chim. Acta*, 2011, **369**, 91–96.

173 L. M. Toma, L. D. Toma, F. S. Delgado, C. Ruiz-Perez, J. Sletten, J. Cano, J. M. Clemente-Juan, F. Lloret and M. Julve, *Coord. Chem. Rev.*, 2006, **250**, 2176–2193.

174 W. F. Yeung, P. H. Lau, T. C. Lau, H. Y. Wei, H. L. Sun, S. Gao, Z. D. Chen and W. T. Wong, *Inorg. Chem.*, 2005, **44**, 6579–6590.

175 J. F. Guo, W. F. Yeung, P. H. Lau, X. T. Wang, S. Gao, W. T. Wong, S. S. Y. Chui, C. M. Che, W. Y. Wong and T. C. Lau, *Inorg. Chem.*, 2010, **49**, 1607–1614.

176 J. Xiang, L. H. Jia, W. L. Man, K. Qian, S. M. Yiu, G. H. Lee, S. M. Peng, S. Gao and T. C. Lau, *Chem. Commun.*, 2011, **47**, 8694–8696.

177 Z. H. Ni, H. Z. Kou, L. F. Zhang, C. H. Ge, A. L. Cui, R. J. Wang, Y. D. Li and O. Sato, *Angew. Chem., Int. Ed.*, 2005, **44**, 7742–7745.

178 Z. H. Ni, L. F. Zhang, V. Tangoulis, W. Wernsdorfer, A. L. Cui, O. Sato and H. Z. Kou, *Inorg. Chem.*, 2007, **46**, 6029–6037.

179 C. F. Wang, J. L. Zuo, B. M. Bartlett, Y. Song, J. R. Long and X. Z. You, *J. Am. Chem. Soc.*, 2006, **128**, 7162–7163.

180 S. Wang, J. L. Zuo, H. C. Zhou, H. J. Choi, Y. X. Ke, J. R. Long and X. Z. You, *Angew. Chem., Int. Ed.*, 2004, **43**, 5940–5943.

181 D. F. Li, S. Parkin, G. B. Wang, G. T. Yee, A. V. Prosvirin and S. M. Holmes, *Inorg. Chem.*, 2005, **44**, 4903–4905.

182 C. F. Wang, W. Liu, Y. Song, X. H. Zhou, J. L. Zuo and X. Z. You, *Eur. J. Inorg. Chem.*, 2008, 717–727.

183 D. F. Li, R. Clérac, S. Parkin, G. B. Wang, G. T. Yee and S. M. Holmes, *Inorg. Chem.*, 2006, **45**, 5251–5253.

184 D. Y. Wu, Y. J. Zhang, W. Huang and O. Sato, *Dalton Trans.*, 2010, **39**, 5500–5503.

185 Y. Zhang, U. P. Mallik, N. Rath, G. T. Yee, R. Clérac and S. M. Holmes, *Chem. Commun.*, 2010, **46**, 4953–4955.

186 Y. Z. Zhang, U. P. Mallik, R. Clérac, N. P. Rath and S. M. Holmes, *Chem. Commun.*, 2011, **47**, 7194–7196.

187 Y. Z. Zhang, U. P. Mallik, N. P. Rath, R. Clérac and S. M. Holmes, *Inorg. Chem.*, 2011, **50**, 10537–10539.

188 B. M. Bartlett, T. D. Harris, M. W. DeGroot and J. R. Long, *Z. Anorg. Allg. Chem.*, 2007, **633**, 2380–2385.

189 E. J. Schelter, A. V. Prosvirin and K. R. Dunbar, *J. Am. Chem. Soc.*, 2004, **126**, 15004–15005.

190 A. V. Palii, S. M. Ostrovsky, S. I. Klokishner, B. S. Tsukerblat, E. J. Schelter, A. Prosvirin and K. R. Dunbar, *Inorg. Chim. Acta*, 2007, **360**, 3915–3924.

191 F. Karadas, C. Avendano, M. G. Hilfiger, A. V. Prosvirin and K. R. Dunbar, *Dalton Trans.*, 2010, **39**, 4968–4977.

192 E. J. Schelter, F. Karadas, C. Avendano, A. V. Prosvirin, W. Wernsdorfer and K. R. Dunbar, *J. Am. Chem. Soc.*, 2007, **129**, 8139–8149.

193 K. R. Dunbar, E. J. Schelter, A. V. Palii, S. M. Ostrovsky, V. Y. Mirovitskii, J. M. Hudson, M. A. Omari, S. I. Klokishner and B. S. Tsukerblat, *J. Phys. Chem. A*, 2003, **107**, 11102–11111.

194 C. G. F. von Richthofen, A. Stammler, H. Bogge, M. W. DeGroot, J. R. Long and T. Glaser, *Inorg. Chem.*, 2009, **48**, 10165–10176.

195 P. J. Ferko and S. M. Holmes, *Curr. Inorg. Chem.*, 2013, **3**, 172–193.

196 D. F. Li, S. Parkin, G. B. Wang, G. T. Yee, R. Clérac, W. Wernsdorfer and S. M. Holmes, *J. Am. Chem. Soc.*, 2006, **128**, 4214–4215.

197 Z. G. Gu, W. Liu, Q. F. Yang, X. H. Zhou, J. L. Zuo and X. Z. You, *Inorg. Chem.*, 2007, **46**, 3236–3244.

198 D. Li, S. Parkin, R. Clérac and S. M. Holmes, *Inorg. Chem.*, 2006, **45**, 7569–7571.

199 K. Mitsumoto, H. Nishikawa, G. N. Newton and H. Oshio, *Dalton Trans.*, 2012, **41**, 13601–13608.

200 J. Y. Yang, M. P. Shores, J. J. Sokol and J. R. Long, *Inorg. Chem.*, 2003, **42**, 1403–1419.

201 D. Li, R. Clérac, O. Roubeau, E. Harté, C. Mathonière, R. Le Bris and S. M. Holmes, *J. Am. Chem. Soc.*, 2007, **130**, 252–258.

202 N. Hoshino, Y. Sekine, M. Nihei and H. Oshio, *Chem. Commun.*, 2010, **46**, 6117–6119.

203 Y.-Z. Zhang, U. P. Mallik, R. Clérac, N. P. Rath and S. M. Holmes, *Polyhedron*, 2013, **52**, 115–121.

204 Y.-H. Peng, Y.-F. Meng, L. Hu, Q.-X. Li, Y.-Z. Li, J.-L. Zuo and X.-Z. You, *Inorg. Chem.*, 2010, **49**, 1905–1912.

205 W. Liu, C.-F. Wang, Y.-Z. Li, J.-L. Zuo and X.-Z. You, *Inorg. Chem.*, 2006, **45**, 10058–10065.

206 L.-C. Kang, M.-X. Yao, X. Chen, Y.-Z. Li, Y. Song, J.-L. Zuo and X.-Z. You, *Dalton Trans.*, 2011, **40**, 2204–2212.

207 D. Li, R. Clérac, G. Wang, G. T. Yee and S. M. Holmes, *Eur. J. Inorg. Chem.*, 2007, **2007**, 1341–1346.

208 Y.-Z. Zhang, U. P. Mallik, R. Clérac, N. P. Rath and S. M. Holmes, *Chem. Commun.*, 2011, **47**, 7194–7196.

209 Y. Z. Zhang, D. F. Li, R. Clérac, M. Kalisz, C. Mathonière and S. M. Holmes, *Angew. Chem., Int. Ed.*, 2010, **49**, 3752–3756.

210 D. Siretanu, D. F. Li, L. Buisson, D. M. Bassani, S. M. Holmes, C. Mathonière and R. Clérac, *Chem.-Eur. J.*, 2011, **17**, 11704–11708.

211 G. N. Newton, M. Nihei and H. Oshio, *Eur. J. Inorg. Chem.*, 2011, 3031–3042.

212 J. Mercurol, Y. L. Li, E. Pardo, O. Risset, M. Seuleiman, H. Rousseliere, R. Lescouëzec and M. Julve, *Chem. Commun.*, 2010, **46**, 8995–8997.

213 A. Mondal, Y. Li, M. Seuleiman, M. Julve, L. Toupet, M. Buron-Le Cointe and R. Lescouëzec, *J. Am. Chem. Soc.*, 2013, **135**, 1653–1656.

214 M. Nihei, Y. Sekine, N. Suganami and H. Oshio, *Chem. Lett.*, 2010, **39**, 978–979.

215 M. Nihei, Y. Sekine, N. Suganami, K. Nakazawa, A. Nakao, H. Nakao, Y. Murakami and H. Oshio, *J. Am. Chem. Soc.*, 2011, **133**, 3592–3600.

216 M. Nihei, Y. Okamoto, Y. Sekine, N. Hoshino, T. Shiga, I. P.-C. Liu and H. Oshio, *Angew. Chem., Int. Ed.*, 2012, **51**, 6361–6364.

217 Z.-H. Ni, H.-Z. Kou, L.-F. Zhang, W.-W. Ni, Y.-B. Jiang, A.-L. Cui, J. Ribas and O. Sato, *Inorg. Chem.*, 2005, **44**, 9631–9633.

218 J. I. Kim, H. S. Yoo, E. K. Koh and C. S. Hong, *Inorg. Chem.*, 2007, **46**, 10461–10463.

219 J. I. Kim, J. H. Yoon, H. Y. Kwak, E. K. Koh and C. S. Hong, *Eur. J. Inorg. Chem.*, 2008, **2008**, 2756–2763.

220 J. I. Kim, H. Y. Kwak, J. H. Yoon, D. W. Ryu, I. Y. Yoo, N. Yang, B. K. Cho, J.-G. Park, H. Lee and C. S. Hong, *Inorg. Chem.*, 2009, **48**, 2956–2966.



221 M. Atanasov, P. Comba and S. Helmle, *Inorg. Chem.*, 2012, **51**, 9357–9368.

222 A. Panja, P. Guionneau, I.-R. Jeon, S. M. Holmes, R. Clérac and C. Mathonière, *Inorg. Chem.*, 2012, **51**, 12350–12359.

223 R. Lescouec, J. Vaissermann, L. M. Toma, R. Carrasco, F. Lloret and M. Julve, *Inorg. Chem.*, 2004, **43**, 2234–2236.

224 T. Senapati, C. Pichón, R. Ababei, C. Mathonière and R. Clérac, *Inorg. Chem.*, 2012, **51**, 3796–3812.

225 S. A. Sulway, R. A. Layfield, F. Tuna, W. Wernsdorfer and R. E. P. Winpenny, *Chem. Commun.*, 2012, **48**, 1508–1510.

226 M. Mousavi, V. Bereau, C. Desplanches, C. Duhayon and J. P. Sutter, *Chem. Commun.*, 2010, **46**, 7519–7521.

227 R. González, A. Acosta, R. Chiozzone, C. Kremer, D. Armentano, G. De Munno, M. Julve, F. Lloret and J. Faus, *Inorg. Chem.*, 2012, **51**, 5737–5747.

228 J. Xiang, L. H. Jia, W. L. Man, K. Qian, G. H. Lee, S. M. Peng, S. M. Yiu, S. Gao and T. C. Lau, *Dalton Trans.*, 2012, **41**, 5794–5798.

229 F. Pointillart, K. Bernot, R. Sessoli and D. Gatteschi, *Inorg. Chem.*, 2010, **49**, 4355–4361.

230 K. S. Pedersen, J. Dreiser, M. Schau-Magnussen, C. A. Thuesen, H. Weihe and J. Bendix, *Polyhedron*, 2012, **46**, 47–52.

231 C. A. Thuesen, K. S. Pedersen, M. Schau-Magnussen, M. Evangelisti, J. Vibenholt, S. Piligkos, H. Weihe and J. Bendix, *Dalton Trans.*, 2012, **41**, 11284–11292.

232 T. Birk, K. S. Pedersen, C. A. Thuesen, T. Weyhermüller, M. Schau-Magnussen, S. Piligkos, H. Weihe, S. Mossin, M. Evangelisti and J. Bendix, *Inorg. Chem.*, 2012, **51**, 5435–5443.

233 J. Dreiser, K. S. Pedersen, C. Piamonteze, S. Rusponi, Z. Salman, M. E. Ali, M. Schau-Magnussen, C. A. Thuesen, S. Piligkos, H. Weihe, H. Mutka, O. Waldmann, P. Oppeneer, J. Bendix, F. Nolting and H. Brune, *Chem. Sci.*, 2012, **3**, 1024–1032.

234 T. Birk, K. S. Pedersen, S. Piligkos, C. A. Thuesen, H. Weihe and J. Bendix, *Inorg. Chem.*, 2011, **50**, 5312–5314.

235 S. K. Singh, K. S. Pedersen, M. Sigrist, C. A. Thuesen, M. Schau-Magnussen, H. Mutka, S. Piligkos, H. Weihe, G. Rajaraman and J. Bendix, *Chem. Commun.*, 2013, **49**, 5583–5585.

236 K. S. Pedersen, G. Lorusso, J. J. Morales, T. Weyhermüller, S. Piligkos, S. K. Singh, D. Larsen, M. Schau-Magnussen, G. Rajaraman, M. Evangelisti and J. Bendix, *Angew. Chem., Int. Ed.*, 2014, **53**, 2394–2397.

237 S. L. Benjamin, W. Levason and G. Reid, *Chem. Soc. Rev.*, 2013, **42**, 1460–1499.

238 H. Tamaki, Z. J. Zhong, N. Matsumoto, S. Kida, M. Koikawa, N. Achiwa, Y. Hashimoto and H. Okawa, *J. Am. Chem. Soc.*, 1992, **114**, 6974–6979.

239 R. Chiozzone, R. González, C. Kremer, G. De Munno, J. Cano, F. Lloret, M. Julve and J. Faus, *Inorg. Chem.*, 1999, **38**, 4745–4752.

240 J. Martínez-Lillo, D. Armentano, G. De Munno, W. Wernsdorfer, M. Julve, F. Lloret and J. Faus, *J. Am. Chem. Soc.*, 2006, **128**, 14218–14219.

241 J. Martínez-Lillo, D. Armentano, G. De Munno, W. Wernsdorfer, J. M. Clemente-Juan, J. Krzystek, F. Lloret, M. Julve and J. Faus, *Inorg. Chem.*, 2009, **48**, 3027–3038.

242 J. Martínez-Lillo, T. F. Mastropietro, E. Lhotel, C. Paulsen, J. Cano, G. De Munno, J. Faus, F. Lloret, M. Julve, S. Nellutla and J. Krzystek, *J. Am. Chem. Soc.*, 2013, **135**, 13737–13748.

243 J. Martínez-Lillo, L. Canadillas-Delgado, J. Cano, F. Lloret, M. Julve and J. Faus, *Chem. Commun.*, 2012, **48**, 9242–9244.

244 J. Vallejo, I. Castro, J. Ferrando-Soria, M. D. Deniz-Hernandez, C. Ruiz-Perez, F. Lloret, M. Julve, R. Ruiz-Garcia and J. Cano, *Inorg. Chem.*, 2011, **50**, 2073–2075.

245 B. J. Kennedy and K. S. Murray, *Inorg. Chem.*, 1985, **24**, 1552–1557.

246 Z. L. Lu, M. Yuan, F. Pan, S. Gao, D. Q. Zhang and D. B. Zhu, *Inorg. Chem.*, 2006, **45**, 3538–3548.

247 L. Lecren, W. Wernsdorfer, Y. G. Li, A. Vindigni, H. Miyasaka and R. Clérac, *J. Am. Chem. Soc.*, 2007, **129**, 5045–5051.

248 R. Ababei, C. Pichón, O. Roubeau, Y.-G. Li, N. Bréfuel, L. Buisson, P. Guionneau, C. Mathonière and R. Clérac, *J. Am. Chem. Soc.*, 2013, **135**, 14840–14853.

249 R. Ababei, Y. G. Li, O. Roubeau, M. Kalisz, N. Bréfuel, C. Coulon, E. Harté, X. T. Liu, C. Mathonière and R. Clérac, *New J. Chem.*, 2009, **33**, 1237–1248.

250 H. Miyasaka, N. Matsumoto, H. Okawa, N. Re, E. Gallo and C. Floriani, *J. Am. Chem. Soc.*, 1996, **118**, 981–994.

251 W.-W. Ni, Z.-H. Ni, A.-L. Cui, X. Liang and H.-Z. Kou, *Inorg. Chem.*, 2007, **46**, 22–33.

252 X. T. Liu, O. Roubeau and R. Clérac, *C. R. Chim.*, 2008, **11**, 1182–1191.

253 J. H. Yoon, J. H. Lim, H. C. Kim and C. S. Hong, *Inorg. Chem.*, 2006, **45**, 9613–9615.

254 H. Miyasaka, T. Nezu, K. Sugimoto, K.-i. Sugiura, M. Yamashita and R. Clérac, *Inorg. Chem.*, 2004, **43**, 5486–5488.

255 H. Miyasaka, T. Nezu, K. Sugimoto, K. Sugiura, M. Yamashita and R. Clérac, *Chem.-Eur. J.*, 2005, **11**, 1592–1602.

256 C. Kachi-Terajima, H. Miyasaka, A. Saitoh, N. Shirakawa, M. Yamashita and R. Clérac, *Inorg. Chem.*, 2007, **46**, 5861–5872.

257 C. Kachi-Terajima, H. Miyasaka, K.-i. Sugiura, R. Clérac and H. Nojiri, *Inorg. Chem.*, 2006, **45**, 4381–4390.

258 J. Cirera, E. Ruiz, S. Alvarez, F. Neese and J. Kortus, *Chem.-Eur. J.*, 2009, **15**, 4078–4087.

259 Y.-Y. Zhu, C. Cui, Y.-Q. Zhang, J.-H. Jia, X. Guo, C. Gao, K. Qian, S.-D. Jiang, B.-W. Wang, Z.-M. Wang and S. Gao, *Chem. Sci.*, 2013, **4**, 1802–1806.

260 R. Sessoli and A. K. Powell, *Coord. Chem. Rev.*, 2009, **293**, 2328–2341.

261 G. Cucinotta, M. Perfetti, J. Luzon, M. Etienne, P. E. Car, A. Caneschi, G. Calvez, K. Bernot and R. Sessoli, *Angew. Chem., Int. Ed.*, 2012, **51**, 1606–1610.

262 N. F. Chilton, D. Collison, E. J. McInnes, R. E. Winpenny and A. Soncini, *Nat. Commun.*, 2013, **4**, 2551.

263 D. Aravena and E. Ruiz, *Inorg. Chem.*, 2013, **52**, 13770–13778.

264 M. Holynska, D. Premuzic, I. R. Jeon, W. Wernsdorfer, R. Clérac and S. Dehnen, *Chem.-Eur. J.*, 2011, **17**, 9605–9610.

265 R. J. Blagg, C. A. Muryn, E. J. L. McInnes, F. Tuna and R. E. P. Winpenny, *Angew. Chem., Int. Ed.*, 2011, **50**, 6530–6533.

266 R. J. Blagg, F. Tuna, E. J. L. McInnes and R. E. P. Winpenny, *Chem. Commun.*, 2011, **47**, 10587–10589.

267 J. D. Rinehart and J. R. Long, *Chem. Sci.*, 2011, **2**, 2078–2085.

268 J. Luzon and R. Sessoli, *Dalton Trans.*, 2012, **41**, 13556–13567.

269 F. Habib, P. H. Lin, J. Long, I. Korobkov, W. Wernsdorfer and M. Murugesu, *J. Am. Chem. Soc.*, 2011, **133**, 8830–8833.

270 A. M. Madalan, N. Avarvari, M. Fournigue, R. Clérac, L. F. Chibotaru, S. Clima and M. Andruh, *Inorg. Chem.*, 2008, **47**, 940–950.

271 M. A. Palacios, A. J. Mota, J. Ruiz, M. M. Hänninen, R. Sillanpää and E. Colacio, *Inorg. Chem.*, 2012, **51**, 7010–7012.

272 G. Poneti, K. Bernot, L. Bogani, A. Caneschi, R. Sessoli, W. Wernsdorfer and D. Gatteschi, *Chem. Commun.*, 2007, **1807**–1809.

273 K. Bernot, F. Pointillart, P. Rosa, M. Etienne, R. Sessoli and D. Gatteschi, *Chem. Commun.*, 2010, **46**, 6458–6460.

274 X. Yi, K. Bernot, F. Pointillart, G. Poneti, G. Calvez, C. Daiguebonne, O. Guillou and R. Sessoli, *Chem.-Eur. J.*, 2012, **18**, 11379–11387.

275 Y. Ma, G.-F. Xu, X. Yang, L.-C. Li, J. Tang, S.-P. Yan, P. Cheng and D.-Z. Liao, *Chem. Commun.*, 2010, **46**, 8264–8266.

276 F. Mori, T. Ishida and T. Nogami, *Polyhedron*, 2005, **24**, 2588–2592.

277 F. Mori, T. Nyui, T. Ishida, T. Nogami, K.-Y. Choi and H. Nojiri, *J. Am. Chem. Soc.*, 2006, **128**, 1440–1441.

278 T. Yamaguchi, Y. Sunatsuki, H. Ishida, M. Kojima, H. Akashi, N. Re, N. Matsumoto, A. Pochaba and J. Mroziński, *Inorg. Chem.*, 2008, **47**, 5736–5745.

279 J.-P. Costes, S. Shova and W. Wernsdorfer, *Dalton Trans.*, 2008, 1843–1849.

280 M. Ferbinteanu, T. Kajiwara, K. Y. Choi, H. Nojiri, A. Nakamoto, N. Kojima, F. Cimpoesu, Y. Fujimura, S. Takaishi and M. Yamashita, *J. Am. Chem. Soc.*, 2006, **128**, 9008–9009.

281 F. Pointillart, K. Bernot, R. Sessoli and D. Gatteschi, *Chem.-Eur. J.*, 2007, **13**, 1602–1609.

282 G.-F. Xu, P. Gamez, J. Tang, R. Clérac, Y.-N. Guo and Y. Guo, *Inorg. Chem.*, 2012, **51**, 5693–5698.

283 G.-F. Xu, Q.-L. Wang, P. Gamez, Y. Ma, R. Clérac, J. Tang, S.-P. Yan, P. Cheng and D.-Z. Liao, *Chem. Commun.*, 2010, **46**, 1506–1508.

284 A. McRobbie, A. R. Sarwar, S. Yeninas, H. Nowell, M. L. Baker, D. Allan, M. Luban, C. A. Muryn, R. G. Pritchard, R. Prozorov, G. A. Timco, F. Tuna, G. F. S. Whitehead and R. E. P. Winpenny, *Chem. Commun.*, 2011, **47**, 6251–6253.



285 J. D. Rinehart, T. D. Harris, S. A. Kozimor, B. M. Bartlett and J. R. Long, *Inorg. Chem.*, 2009, **48**, 3382–3395.

286 J. D. Rinehart and J. R. Long, *Dalton Trans.*, 2012, **41**, 13572–13574.

287 J. D. Rinehart and J. R. Long, *J. Am. Chem. Soc.*, 2009, **131**, 12558–12559.

288 M. A. Antunes, L. C. J. Pereira, I. C. Santos, M. Mazzanti, J. Marçalo and M. Almeida, *Inorg. Chem.*, 2011, **50**, 9915–9917.

289 J. D. Rinehart, K. R. Meihaus and J. R. Long, *J. Am. Chem. Soc.*, 2010, **132**, 7572–7573.

290 J. T. Coutinho, M. A. Antunes, L. C. J. Pereira, H. Bolvin, J. Marçalo, M. Mazzanti and M. Almeida, *Dalton Trans.*, 2012, **41**, 13568–13571.

291 F. Moro, D. P. Mills, S. T. Liddle and J. van Slageren, *Angew. Chem., Int. Ed.*, 2013, **52**, 3430–3433.

292 N. Magnani, C. Apostolidis, A. Morgenstern, E. Colineau, J.-C. Griveau, H. Bolvin, O. Walter and R. Caciuffo, *Angew. Chem., Int. Ed.*, 2011, **50**, 1696–1698.

293 D. P. Mills, F. Moro, J. McMaster, J. van Slageren, W. Lewis, A. J. Blake and S. T. Liddle, *Nat. Chem.*, 2011, **3**, 454–460.

294 V. Mougel, L. Chatelain, J. Pécaut, R. Caciuffo, E. Colineau, J.-C. Griveau and M. Mazzanti, *Nat. Chem.*, 2012, **4**, 1011–1017.

295 S. M. Cornet, L. J. L. Haller, M. J. Sarsfield, D. Collison, M. Helliwell, I. May and N. Kaltsoyannis, *Chem. Commun.*, 2009, 917–919.

